Insulating Biomaterials N01-NS-2-2347

First Quarterly Progress Report October-December, 2002

National Institutes of Health

National Institute of Neurological Disorders and Stroke

Neural Prosthesis Program

InnerSea Technology

1 DeAngelo Drive
Bedford, MA 01730

Contributors:

Dave Edell, PI

Bill Mather, IC Design

Robyn Edell, Testing

Sean Sexton, Instrumentation and Software

Ying-Ping Liu, Assembly and Testing

Karen Gleason, Chem Eng (MIT)

Shannan O'Shaughnessy, Grad Student, Chem Eng (MIT)

Objectives

The goal of the Insulating Biomaterials work is to identify and evaluate materials, coatings, and assembly techniques suitable for protection of integrated circuit devices being considered for neural prosthetic applications. A lifetime design goal of 100 years of *in-vivo* functionality will provide a reasonable margin of safety for materials defined by this program. A multi-faceted research program is proposed to allow investigation of known failure mechanisms of the materials and techniques under study as well as the discovery of new failure mechanisms. Both *in-vivo* and *in-vivo* testing will be used with a variety of testing procedures, devices, and materials to further discover, develop and understand insulating biomaterials for micro-machined devices.

From past experience, silicones and fluoropolymers are the most likely materials to withstand the *in-vivo* environment for many decades and provide high level insulation properties throughout. Liquid Crystal Polymer (LCP) is a relatively new material which when produced correctly exhibits near hermetic qualities. It is a polymer similar in feel to Mylar which is dimensionally stable and thus can be patterned with thin film metals for circuits or interconnects. LCP is also biocompatible and inexpensive. Thus thorough evaluation of LCP is a main focus of the proposed work. Other materials will also be tested as they become available. One objective of expanding our instrumentation is to allow for a wider variety of materials under test in addition to allowing testing in a variety of *in-vitro* environments. Accordingly, we accept as many new materials as possible from others for testing in our systems.

The objectives of *in-vitro* testing are to minimize the use of animals by cost effective rapid screening of materials under consideration prior to implantation, and to identify possible failure mechanisms using accelerated testing by various techniques including: 1) sensitive measurements; 2) sensitive test devices; 3) elevated temperature; 4) chemical concentration enhancements; 5) mechanical stress; and 6) electrical stress. *In-vitro* evaluations will be accomplished under

conditions similar in simple ways to physiological conditions so that results can be more readily understood in terms of the properties of the materials.

There are three specific objectives for *in-vivo* testing. One is to directly evaluate candidate materials from the *in-vitro* testing in mammalian brain which is a more realistic test environment than *in-vitro* testing can ever be. A second objective of *in-vivo* testing is to discover new possible failure mechanisms that can then be used to augment the *in-vitro* testing by allowing acceleration of specific biologically related failure mechanisms. The third objective is to provide a realistic application environment to help uncover issues that have not yet been addressed.

Another aspect to the proposed program is the testing and evaluation of other parameters that may be related to degradation processes of interest. One such example is the measurement of peel force to determine interfacial bond strength between insulators and the surfaces they are to protect. Another is the measurement of elasticity which may show changes in cross link density of a material that could lead to material weakening and eventual failure.

Another objective of the proposed work is to develop and evaluate new materials and application techniques specifically designed for implantable micromachined CMOS integrated circuits useful in neuroprostheses and other medical applications. While we capitalize on the developments from other fields of insulating materials that happen to be biocompatible from other fields, this portion of the work focuses on development of coatings for this specific application. Most of this effort will be focused on Chemical Vapor Deposition techniques in order to develop thin, conformal coatings for the complex geometries of wire bonded, micro-machined silicon devices. However, some effort will be directed towards improving the characteristics of silicones used for encapsulation of implantable CMOS integrated circuits.

The final and most important objective is to develop procedures for routine assembly of implantable CMOS integrated circuits that can be implanted with

confidence that they will survive the sub-dural or intra-cortical environment for many decades. These assembly procedures are involve a great many details from maintaining a clean, Electro Static Discharge (ESD) safe environment to which flux is most compatible with existing cleaning procedures. Device cleaning prior to encapsulation is of major importance to the success of any long term implant. Development and validation of cleaning procedures is a major focus of this proposed work. The *in-vivo* test environment for a completed device is a biochemically rich matrix of solvents, acids, bases, enzymes, that is in constant micro and macro motion. While we may never fully understand all that occurs in the *in-vivo* environment, it is crucial that the devices under study be subjected to this environment to complete the evaluations.

Short Summary of Work in Progress

Long term soak testing of samples retained from the previous contract are continuing. As devices fail, the failure is verified by manual measurements to confirm the readings from the automated system. Peel testing is continuing with an emphasis on refining the technique to yield reproducible results. To date, there is an order of magnitude variation at times between samples prepared as identically as possible. Uptake studies are continuing in search of biochemicals that may be significant in the aging of silicones within biological environments. New LCP substrates were designed and submitted for fabrication. Free running charge integrator arrays were received back from MOSIS and were tested showing excellent characteristics so far. Alternative designs, based on commercially available devices are being explored to reduce the overall cost of the new system. Failed implant telemeters are being removed and evaluated.

Book Chapter

Appended is a chapter on Insulating Biomaterials submitted for a book on neuroprostheses titled “Neuroprostheses: Theory and Practice” (Horch and Dhillon, eds). This chapter is a relatively recent compilation of much of the insulating biomaterials work being conducted under this contract.

Chapter 3.2

Insulating Biomaterials

David J. Edell
Innersea Technology, One DeAngelo Drive, Bedford, Massachusetts 01730
E-mail: djedell@innersea.com

Abstract

Implantable devices for neuroprostheses should be as small as possible to minimize damage to target neural structures. Silicon integrated circuit and micromachining technology has enabled fabrication of very small, electrode arrays and complex electrical systems. However, application of this advanced technology requires development of new insulating materials for operation of theses electronic devices within the conductive, aqueous environment of animals and humans. These insulating biomaterials must be "biocompatible" (cause no foreign body response from the host) and "bioresistant" (remain unaffected by the host environment) from a few months up to 100 years for various applications. The results described are from "in progress" research under a long standing program funded by the NIH Neuroprosthesis Program. Commercially available and newly synthesized insulating biomaterials are being evaluated using a variety of sensitive measurements and accelerated degradation techniques. Wire insulators, ribbon cable interconnect insulators, silicon device surface encapsulants, encapsulants for alumina and quartz hybrid circuit substrates and assemblies, and encapsulants for silicon CMOS integrated circuit devices are being studied. Surface adhesion, material mechanical properties, and electrical performance, are being evaluated at 37°C, 90°C, and *in-vivo*. Silicones and fluoropolymers are the most stable materials yet studied.

1. Introduction

Implantable micro-devices based on silicon micro-technology are a promising new class of medical devices that may find important applications in medicine and particularly in rehabilitation. In order to use silicon micro-technology for clinical devices, it is necessary to develop thin, electrically insulating material coverings that will protect such devices from the conductive, corrosive environment of the body for many decades. The goal of a long standing NIH program on "Insulating Biomaterials" has been to develop and evaluate such coverings for a projected lifetime of 100 years[30].

1.1. History of insulating biomaterials

Insulating biomaterials research has been underway for many decades to support technological innovations in implantable electronics such as the cardiac pacer and the cochlear prosthesis. Microelectronic components and integrated circuits have been used extensively in cardiac pacing and cochlear prosthesis implant systems. Both of these systems typically utilize large titanium or ceramic canisters for packaging the electronics, and glass feedthroughs for interconnecting with stimulation leads and electrodes. The pace of development of these implantable devices has paralleled the pace of technological innovation. Development of the cardiac pacemaker is a very good example. The first recorded demonstration of electrical pacing of the heart occurred in 1872 using a system consisting of a 300 V battery and hand held electrodes[38]. Following that important demonstration, it wasn't until endomysial electrodes, transistors, epoxy encapsulation, and high energy density batteries became available in the 1950s that the stage was set for development of the fully implantable cardiac pacemaker reported in 1960[8]. In the 1970s, titanium casings replaced epoxy encapsulation which allowed incorporation of integrated circuits based on silicon microelectronics technology. Lithium batteries, improved packaging, and improved lead technology resulted in complex pacemaker systems with implantable lifetimes of up to 15 years[36].

Today's pacemakers consist of lithium-ion batteries and electronics modules hermetically sealed within titanium canisters using glass insulated and sealed electrical feedthroughs. The size of the pacemaker is dominated by the size of the battery and the titanium case which is a few centimeters in

diameter and a half centimeter thick. Modern leads are typically multi-filament coils of a high nickel content stainless steel alloy (MP35N) insulated with silicone elastomer.

Throughout the history of the pacing industry, implantable materials considerations have dominated technological innovation. Silicone insulated leads have been very reliable and have been used for decades in cardiac pacing applications. Other lead insulation materials have been used to overcome the tendency of silicones to stick to tissue during insertion, and to reduce the diameter of the pacing lead[36]. Polyurethanes used for this application were marketed in the 1970s. However, in several long term clinical studies, polyurethane leads from several manufacturers tragically exhibited substantially higher failure rates than silicone leads[40,57]. A possibly overlooked clue that may have alerted lead designers to possible long term instability issues with polyurethanes was the 1979 observation that both polyether and especially polyester urethanes were susceptible to hydrolytic degradation during relatively short term water soak[43].

The most important goal of current work on insulating biomaterials is to identify possible failure modes for insulating biomaterials to avoid such clinical surprises. Many applications for implantable microelectronics and micromachined devices are under development including biochemical sensors and drug delivery systems. Most of these applications require only subcutaneous implantation so the traditional titanium canister is the package of choice. Neuroprostheses, however, require implantation of devices within the nervous system.

1.2. Insulating biomaterials for neuroprostheses

Neuroprostheses are being developed for rehabilitation of the deaf, blind, spinal cord injured, and amputees. Most of the neuroprostheses concepts require close proximity to the small (10 µm nominally) and fragile cells of the nervous system. Many will be attached or embedded directly in neural tissue. Not only is neural tissue tightly packed with functional elements, but also it is dynamic. Peripheral nerves stretch and relax with every motion of a limb. The spinal cord moves within the spinal canal stretching the spinal roots with every bend. The brain moves relative to the skull with every heartbeat, breath, and motion of the head. Eyes are constantly in motion creating substantial forces of acceleration on the retina and bending and stretching of the optic nerve.

Because of the biological environment, the fragile nature of neural tissue, the tight packing density of neurons, the relative motions of tissues, and the effects of acceleration, an implantable electronic device for neuroprostheses should have the following characteristics for optimal performance:

- biocompatibility
- bioresistance
- small size
- density and stiffness equal to that of neural tissue
- minimal tethering to adjacent structures

Biocompatibility is essential to minimize formation of connective tissue between neurons and electrodes over the course of long-term implantation. Bioresistance ensures that the implanted electronic device remains functional for decades. Small size (measured in micrometers) is necessary to minimize damage to target neural structures during placement and to allow devices to fit into small spaces without damaging adjacent tissue. Matching the density and stiffness of the device to neural tissue is important to avoid damage to the device or tissue from differential acceleration and distortion caused by intrinsic motion of the tissue, as well as from extrinsic accelerations caused by normal motion or traumatic incidents. Tethering is usually created by the interconnect between a skull or skin mounted connector, or an implanted battery or telemetry package, and the implanted device. The connectors or large packages provide a point of fixation. Minimal tethering reduces the likelihood that forces will be transmitted from a fixation point to the implant during relative motions of the two.

The ideal implantable neuroprosthetic device would thus have: no chemical reactivity (an important aspect of both biocompatibility and bioresistance); zero dimensions to avoid traumatic damage to the target and surrounding tissues; density equal to that of neural tissue to avoid acceleration damage; mechanical properties matched to neural tissue to absorb geometric changes; and no tethering. Devices approximating this ideal are being developed at a variety of locations worldwide using micromachining of silicon as a base technology. Silicon is a good choice since it readily forms an inert, self-limiting oxide that

is biocompatible[32-34]. Silicon micro-machining can be used to produce a variety of novel structures that may approximate the ideal neuroprosthesis[7,28,31-34,41,44,47,48,51,54,62], primarily by making devices that are small.

1.2.1. Silicon micro-machined neuroprostheses

Silicon micro-machined devices typically are not bioresistant. Figure 1 illustrates some possible failure modes when an integrated circuit micro-device is immersed in saline environments for extended periods of time. There are several problem areas associated with operation of micro-fabricated electrical devices within physiological systems.

- Micro-wires used to attach to the device must be capable of withstanding immersion in ionic fluids with a 2–5 V potential across the insulation.
- The exposed areas where the wires are attached to connectors or devices must be coated with a material that is typically applied after bonding has been accomplished.
- Where two surfaces are joined voids in the encapsulant must be avoided, and a hydrolytically stable bond must be achieved.
- The interconnect must be flexible enough to minimize static forces applied by the implanted element on the tissue. Dynamic flexing is small but could contribute to failure in an insulator that has been mechanically weakened by electrochemical attack.
- The integrated circuits on the chip must be protected from water and ionic contamination (i.e. the surface density of sodium ions in the CMOS (Complementary Metal Oxide Semiconductor) gates should be maintained at less than 10^9 cm^{-2}). The device surface materials, where exposed, and encapsulants must be bioresistant and biocompatible. Encapsulated substrate materials must be stable in the presence of water vapor, and must not migrate through encapsulating materials.
- These micro-machined devices will not find useful clinical applications until suitable insulating biomaterials and packaging techniques have been identified for protecting the devices from the environment of the body for many decades while maintaining the advantage of small size.

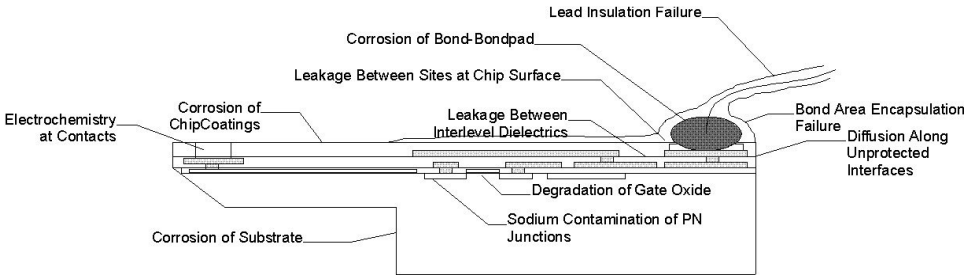

Fig. 1. Sketch illustrating potential problem areas for implantable integrated circuits protected by thin layers of insulating biomaterials.

1.3. Historical failures of insulating biomaterials

While there are many coatings that could be used for insulating electronics and protecting micromachined integrated circuits, few are suitable for direct immersion into biological systems or even aqueous environments. Common materials used successfully by the electronics industry for protecting integrated circuits are not necessarily stable in aqueous environments. This fact is often under-appreciated. Several examples exist of unexpected failures from materials that were not tested under realistic conditions. One example was the extensive use and proposed use of polyimide for development of neuroprostheses. This

choice was based on the experience of the electronics industry, but the material had never been fully evaluated under saline conditions. However, since 1971 it has been known that polyimide is susceptible to hydrolysis[13]. Polyimide also undergoes enhanced degradation in the presence of applied electrical potentials[53]. Parylene-C has also been widely promoted as an insulating biomaterial. While effective for short term encapsulation, Parylene undergoes hydrolysis with resultant craze cracking upon exposure to high humidity[46].

There are other examples of packaging surprises, some with tragic loss of human life, and all very costly to the industry. The important point to be made is that life testing of materials is an art rather than a science. The tragic mistakes are made when too much emphasis is placed on theoretical models of accelerated testing without due consideration for the simplifying assumptions.

1.4. Goals of current insulating biomaterials research

The goal of insulating biomaterials research is to identify and evaluate materials, coatings, and assembly techniques suitable for protection of integrated circuit devices being considered for neural prosthetic applications. A lifetime design goal of 100 years of *in-vivo* functionality was chosen to provide a reasonable margin of safety for materials defined by this program. A multi-faceted research program is being pursued to allow investigation of known failure mechanisms of the materials and techniques under study as well as the discovery of new failure mechanisms. Both *in-vivo* and *in-vivo* testing are being used with a variety of testing procedures, devices, and materials to further discover, develop and understand insulating biomaterials for micromachined devices.

The objectives of *in-vitro* testing are to minimize the use of animals by cost effective rapid screening of materials under consideration, and to identify possible failure mechanisms using accelerated testing by three techniques: 1) sensitive measurement; 2) elevated temperature; and 3) chemical concentration enhancements. *In-vitro* evaluations will be accomplished under conditions similar in simple ways to physiological conditions so that results can be more readily understood in terms of the properties of the materials.

There are two specific objectives for *in-vivo* testing. One is to directly evaluate candidate materials from the *in-vitro* testing in a more realistic test environment for the application - the mammalian brain. A second objective of *in-vivo* testing is to discover new possible failure mechanisms that can then be used to augment the *in-vitro* testing by allowing acceleration of specific biologically related failure mechanisms.

The final objective is to synthesize and evaluate new materials specifically designed for implantable micromachined CMOS integrated circuits useful in neuroprostheses and other medical applications. These new materials are based on chemistries similar to commercially available materials, but synthesized and deposited with techniques consistent with the need for thin film coatings to maintain the size and desired mechanical properties of micromachined sensors. Synthesis of new materials is reported in Chapter 3.3.

2. Approach – *in-vitro* and *in-vivo*

One key question in this work is how long can an encapsulant last that shows no sign of degradation? When there are measurable levels of degradation, curve fitting can be judiciously used to predict the upper bound of device lifetime which may eliminate some materials. However, such testing cannot be used to accept a material that shows no sign of degradation because there may be other factors that have yet to be identified that may not have been revealed. It would be useful to have a method for setting the upper bounds on materials that show no signs of degradation under normal testing. While the best materials may show no direct electrical signs of degradation under any conditions, other measures may provide indicators. For example, elasticity measurements may demonstrate subtle processes in progress that cannot be resolved by other measures. It may be that some materials are more rapidly degraded because they carry a greater percentage of whatever chemical bond is suspected. These materials may be useful in establishing activation energies for use with other materials that have not shown degradation thus far but are known to contain a smaller fraction of the suspected weak link.

If it is assumed that the process being detected can actually cause device failure, an upper estimate of the life of the system can be made. Without an identified trend, it is necessary to determine what the minimum trend is that could be seen with the type of data available. Using regression statistics, a statistically reliable minimum observable slope of changes in the property being measured can be computed. This will be determined by the noise in the data and the sensitivity of the measurements.

2.1. Accelerated testing

Accelerated testing for insulating biomaterials research consists of combinations of accelerated detection and accelerated degradation.

2.1.1. Detection

Accelerated detection depends on development of sensitive test structures as well as sensitive test instrumentation. Devices currently in use for accelerated detection include wire insulation test devices, bulk insulator resistivity monitors, InterDigitated Electrode (IDE) devices, four point resistance monitors, Young's Modulus monitors, and surface bonding monitors.

Insulated wire loops are a convenient way to initially screen materials that may be commercially available as a wire coating. Loops of wires are connected to the electrometer test units and immersed in saline. One end of the loop is usually open circuit and is only used to check integrity of the measurement pathway. The other end of the loop is connected to the feedback node of an electrometer. Bias is provided through a platinum electrode immersed in the saline.

Bare silicon wafers are used to screen materials for bulk resistivity. These devices are fabricated by first coating one surface with the material to be tested, and then attaching a wire to the back surface and potting the assembly leaving a 0.25 in. diameter opening over the material under test. These devices are then immersed in saline for long term testing. Bias is provided through a platinum electrode immersed in the saline. Integrity of the measurement pathway is verified using capacitance measurements between the substrate and saline solution.

Inter-Digitated Electrodes (IDEs) are used to evaluate protection of the surface interface between an encapsulant and substrate. All of the materials tested have at least a native silicon dioxide layer on the surface prior to encapsulation, so it is expected that the silicon dioxide to encapsulant chemical bond integrity is what is being evaluated assuming proper surface cleaning prior to coating. Continuity is monitored by return connections through each electrode of an interdigitated electrode set.

Early IDE structures (called "BondChips") were fabricated of semiconductor silicon with either silicon dioxide or silicon nitride surfaces. The outermost atoms of a silicon nitride surface rapidly changes to silicon dioxide upon exposure to air, so the actual interface being tested is likely the silicon dioxide molecules (assuming the surface has been properly cleaned). Also included were bond sites for assessing the reliability of the wire bond – metal pad interface, metal contacts to a polysilicon resistor and the polysilicon resistor itself.

An early attempt at monitoring CMOS circuit elements resulted in development of gate oxide monitors. These devices were fabricated by the MOSIS, Inc. foundry service. These devices monitored the stored charge on a UV programmable capacitor put in place by a one time programming of a small storage capacitor prior to assembly. However, these devices only provided single point measurements and were susceptible to static electricity discharge of the gate.

To allow more thorough, and long term investigation of CMOS circuit elements, the CMOS circuit test chip introduced above included 14 test devices that allow continuous monitoring of the leakage currents through and between all of the CMOS dielectric layers. Test devices included stacked perforated plates for vertical leakage pathways, IDEs for lateral leakage pathways, large area reverse biased diodes, surface plates for bulk leakage pathway, surface IDEs for encapsulant/chip interfacial leakage pathways, MOS threshold testers, and an uncommitted pad set for attachment of an external IDE or other test structure.

While most of the above test devices will eventually yield solid data that will guide selection of encapsulation materials and methods, results are very slow. Pull tests have been implemented to provide

earlier evidence of material weakening or interfacial adhesion loss in advance of overt electrical failure. Elasticity of encapsulants is monitored using 1 or 2 mm diameter rods of materials of interest in a non-destructive, cyclic pull test. These pull test devices are sensitive to small structural changes in the material that can be caused by cross linking, de-polymerization or other factors. The diameter of the devices is small to promote any diffusion limited processes. These devices are soaked at 90^0C in sterile water to minimize salt crystal deposits that could mechanically cause unnatural degradation. These devices are also readily implanted in the subcutaneous space for long-term *in-vivo* evaluation.

Peel tests are used to determine adhesion failure issues. Simple devices are constructed with a surface and encapsulant where the encapsulant and surface under test are pulled apart incrementally at intervals during soak testing in water. By measuring the force of de-lamination, and monitoring it over time, a rough measure of adhesion is obtained. Adhesion may be affected by chemical degradation of the bond interface by hydrolysis or other chemical reaction or during assembly by incorporation of contaminants at the interface due to improper cleaning procedures. Thus this method can be used as an aide in development of new cleaning procedures that can then be verified using more sensitive but slower methods.

2.1.2. Accelerated degradation

Elevated temperature is an example of a commonly used means of accelerating failure of a material. There are many pitfalls in using heat to accelerate the aging process. One is that the chemical reaction is assumed to be first order. It is necessary to determine the activation energy for the process. There must be no "gettering" processes ongoing, and there cannot be competing reactions with different activation energies that could differentially accelerate thereby changing the nature of the system at different temperatures. Thermal expansion issues should not dominate the results. There probably are other issues as well, but this list is simply intended to inject caution to the interpretation of the high temperature soak data. If the activation energies of the degradation processes are known, the minimum slope at the elevated temperature can be used to provide an indicator of possible lifetime at lower temperature.

While accelerated degradation testing can be used to point out possible failure mechanisms, long term, high sensitivity tests should be conducted in parallel with the accelerated tests to ensure that other factors are not being missed. For example, it is possible that the acceleration factor may also accelerate a repair or stabilization phenomenon that could hide a degradation process. Likewise, under non-accelerated conditions, there may be parallel paths of leakage currents such that a stable, relatively high but acceptable leakage current masks a lower level current that is increasing with time. Until the lower level leakage pathway becomes comparable to the higher leakage path, it cannot be noticed. Merely fitting trends to this data will show early in the process that the device may last indefinitely. However, if observed long enough, or if the process can be thermally accelerated without changing the nature of the processes involved, then eventually the formerly steady leakage observations will suddenly, and unexpectedly change when the hidden process emerges. Last, it is important to consider the possibility that an accelerated test will demonstrate failures where none would exist under normal circumstances. An obvious example of a faulty accelerated test would be to raise the temperature to the combustion point of the material under test. A more subtle example would be to raise the temperature of a sample above the normal use temperature when the sample is composed of materials with substantially different thermal expansion properties.

In addition, it is difficult to devise a general test when the final device configuration is unknown. Simple changes in geometry between the test device and the final device, for example, can alter net diffusion rates which could invalidate a predictive model that does not take geometrical changes into account.

While difficult to interpret, accelerated degradation techniques can still be useful. One approach to accelerated degradation of insulating biomaterials is to test sensors under normal use conditions as well as under conditions of increased stress. Normal use testing allows direct evaluation of potential failures and depends on enhanced sensitivity of the measurements for accelerated detection of normal degradation. Increased stress testing is used to accelerate degradation processes that may then be sensed earlier than at normal use conditions. The results of the accelerated degradation experiments are used to discover various possible failure mechanisms which can then be considered when interpreting data from the long term normal use testing. In addition, results of accelerated degradation experiments can also be useful in

designing new sensors or instrumentation for subsequent testing. However, accelerated degradation experiments should not be used to predict long term results under normal use conditions.

2.1.2.1. Temperature

The classic Arrhenius equation for acceleration of degradation by temperature in a first order chemical reaction or diffusion process is described in Eq. 1[49].

$$K = e^{\frac{E_a}{k}\left[\frac{1}{T_1}-\frac{1}{T_2}\right]} \quad (1)$$

where K = acceleration multiplier, E_a = activation energy (electron volts), k = Boltzman's constant (8.62×10^{-5} eV/°K), $T_{1,2}$ = absolute temperature (°K).

Fig. 2 is a plot of Eq. 1 illustrating the temperature acceleration of a first order process with a nominal activation energy of 1 eV. Since the process kinetics and activation energies are unknown, and are exponentially dependent, this computed data can only serve to indicate an appropriate temperature spread for testing.

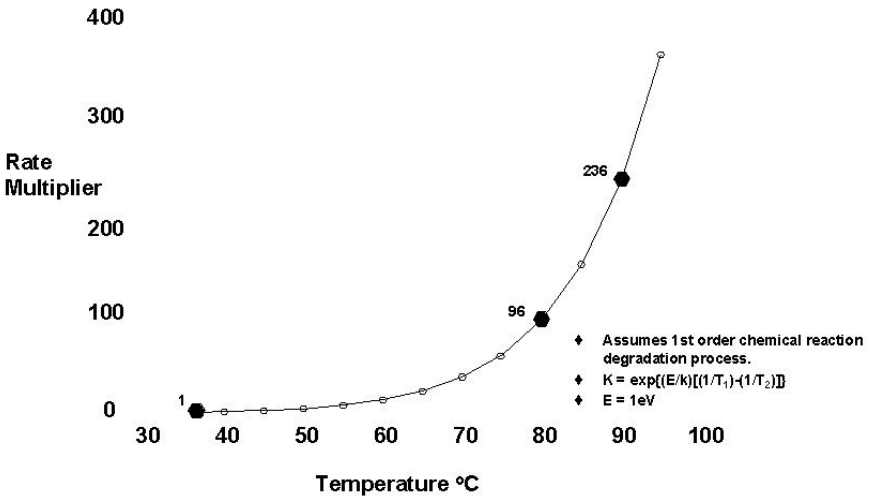

Fig. 2. Plot of Eq. 1 showing acceleration of a first order chemical reaction by to increasing absolute temperature.

Soak temperatures of 37, 80, and 90^{O}C were originally selected, but test space in the instrumentation was limited so only 37 and 90^{O}C were implemented.

2.1.2.2. Mechanical

Implantable micro-devices typically undergo minimal mechanical stress. However, by adding mechanical stress to the measurement and detection routines, it may be possible to detect chemical changes in the material. An example that was cited earlier is the hydrolysis of structural bonds in polyimide which results in lowering of the tensile strength leading to crack formation in the presence of mild mechanical stress. Such effects can be observed by simply bending insulated wires on a specific radius which puts the insulator under both tensile and compressive forces and then soak testing. Since the insulation on the outer

radius is under constant tension, if there is significant mechanical weakening of the material cracks and electrical failure may occur.

2.1.2.3. Chemical

A variety of analytical methods were considered for trying to determine the chemicals responsible for degradation of various materials under test *in-vivo*. However, searching for biochemicals was not feasible when the variety of possibilities is high as found in the chemistry of biological systems. A new approach has been designed which will not use the body as the test vehicle, but rather will use single chemicals known to be part of the biological milieu. Pre-weighed test samples of potential insulating biomaterials can then be immersed in these chemical solutions and weighed on a microbalance periodically to see how much of a particular chemical is taken up. By maintaining a saturated solution of the chemical under test, a constant diffusion gradient should be established which may allow computation of the diffusion coefficient for the contaminant in the insulating biomaterial. Since all of the solutions will have 2 components — solvent and solute, controls measuring the uptake of solvent will also be run, and final samples will be dried prior to weighing to verify the results. These experiments are just being initiated. Once the uptake properties of a particular material are understood, it will then be feasible to look for that chemical following long term immersion in animals. With the major chemicals identified, it may be possible to use *in-vivo* experiments to determine if there are other chemicals not previously identified that have been concentrated in the encapsulants. Eventually, this data will be correlated with long term soak data for mechanical properties changes, peel force changes, and electrical performance changes.

3. Methods

3.1. Designs

A variety of test devices have been developed over the years to investigate different materials and different aspects of materials. Insulated wire loops are a convenient way to initially screen materials that may be commercially available as a wire coating. A voltage bias is impressed across the insulator while leakage currents through the insulators are measured.

Bare silicon wafers are used to screen materials for bulk resistivity. These test devices are fabricated by first coating one surface with the material to be tested, and then attaching a wire to the back surface and potting the assembly leaving a 0.25 in. diameter opening over the material under test. These devices are then immersed in saline for long term testing. As for many of the details in this work, the measurements of these devices are limited in sensitivity by whatever is used to encapsulate the backside. Typically, the best performing encapsulant yet identified is used at the time of assembly.

InterDigitated Electrodes (IDEs) (or “Triple Track Devices”) are used to evaluate protection of the surface interface between an encapsulant and substrate. All of the substrate materials under test have at least a native metal oxide layer on the surface prior to encapsulation. Thus it is the substrate metal oxide surface to encapsulant chemical bond integrity that is being tested. The pitch of the IDEs depends on the technology used to fabricate them. For silicon devices, typical lines and spacings are 2-10 µm. For hybrid circuit substrates lines and spacings are typically 1-3mils. Printed circuit board fabrications are usually limited to 3-5 mils.

Some of the early IDE structures (“BondChips”) included an eight point polysilicon resistor structure that allowed long term monitoring of polycrystalline silicon resistors and contacts. These devices worked well, but were very expensive to fabricate. Devices from the University of Michigan Center for Neural Communication Devices include contact test structures and polysilicon resistors.

Elasticity is monitored using 1 or 2 mm diameter rods of materials of interest in a cyclic pull test. These pull test devices are sensitive to small structural changes in the material that can be caused by cross linking, de-polymerization, infiltration of other materials, or other factors. The diameter of the devices is small to promote any diffusion limited processes.

Peel test devices were developed to allow direct testing of encapsulant - substrate adhesion. These devices and the associated testing were developed to allow relatively rapid testing of adhesion related failure. Peel testing of devices first contaminated with various materials and then cleaned with a variety of cleaning procedures is providing information on what types of contaminants are important concerns, and what cleaning procedures are appropriate. Peel tests may also be valuable for determining the effects of various biochemicals that may diffuse through encapsulants.

Since the ultimate goal is to be able to protect implantable integrated circuits, direct tests of critical elements of silicon integrated circuits were devised. Several oxide monitors were fabricated in MOSIS (a silicon foundry service) which monitored the stored charge on a UV programmable capacitor. This device was to monitor gate oxide leakage currents from a one time programming of a small storage capacitor, but proved difficult to use and interpret in practice because of random discharges of the programmed capacitor, perhaps due to static charge buildup. Further, this expensive, time consuming test device only monitored one aspect of CMOS integrated circuit technology.

To allow more thorough investigation of CMOS circuit elements, particularly *in-vivo,* a CMOS circuit test chip was developed which included 14 test devices for continuous monitoring of the leakage currents through and between all of the CMOS dielectric layers and devices. Test devices included stacked perforated plates for vertical leakage pathways, IDEs for lateral leakage pathways, large area reverse biased diodes, surface plates for bulk leakage, surface IDEs for encapsulant/chip interfacial leakage, MOS threshold testers, and an uncommitted pad set for attachment of an external IDE or other test structure. These devices have integral telemetry to allow implantation in animals for long term testing in the intra-cortical environment.

3.2. Measurement systems

Initially a single channel system based on a Keithley 617 electrometer interfaced to a PC type computer was developed. The focus of the design was to minimize noise while maximizing sensitivity in order to be able to reliably measure resistances on the order of $1x10^{16}\ \Omega$. By automating the data acquisition process, it was possible to use averaging to reduce the overall noise of each data point, and to further reduce the noise by linear regression analysis of the data to extract the effective resistance.

One issue that soon became apparent was that of settling time. While the measurement electronics settled within a few seconds, slow decay of charges that were apparently trapped created tremendous variability from device to device. In addition, noise levels varied considerably from device to device. After much consideration, it was decided to use programming to allow the measurement to settle and to use a statistical endpoint. That is, the definition of "settled" and ready for data acquisition was different for every device and was determined by when the difference between means of two consecutive data grabs was smaller than a fraction of the standard deviation of that data. This worked well. The final choice for the fraction of the standard deviation criterion was a compromise between overall measurement time (a few days per device), and the observed hysteresis in the IV sweep. If the settling time were too short, the hysteresis loop was larger than necessary.

A raw data sweep is shown in Fig. 3. This is from a 60 cm long gold wire with Teflon® insulation. The small hysteresis exhibited here does not affect the linear regression analysis used to assign the apparent resistance since it is symmetrical about the regression fit.

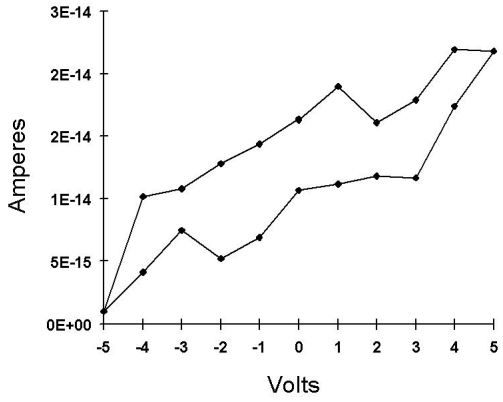

Fig. 3. A-M Systems 3 mil gold wire with 1 mil Teflon®, 60 cm long (~1cm2).

3.2.1. Multi-channel electrometer measurements

Due to the large number of samples under test, and the long settling time for each measurement, a single channel measurement system delayed repeat measurements of devices by several months. High sensitivity computerized instruments and protocols for monitoring leakage currents and resistances were developed for *in-vitro* work. A wide dynamic range 384 channel system was developed for long term measurements. One key feature of the 384 channel electrometer system is that the devices being tested remain continually connected to the instrumentation so measurements can be accomplished every few days. Another key feature is that the devices being measured can be placed in heated environments and connected to the electrometers using simple Teflon® insulated wires that have been found to retain high insulation resistance indefinitely. The third key feature of this relatively new system, and perhaps the most important was the development of a "long tube" test vessel which allows heating test devices immersed in saline or ringer's solution while maintaining the cap, seal, and connector near room temperature as shown in Fig. 4. This avoids the problem with long term degradation of the test unit which was a significant problem for the older devices placed in incubators. Also, because the upper portion is relatively cool, water vapor condenses and falls back into the soak solution. Thus very seldom do these assemblies need to be opened and filled which minimizes breakage as well as time.

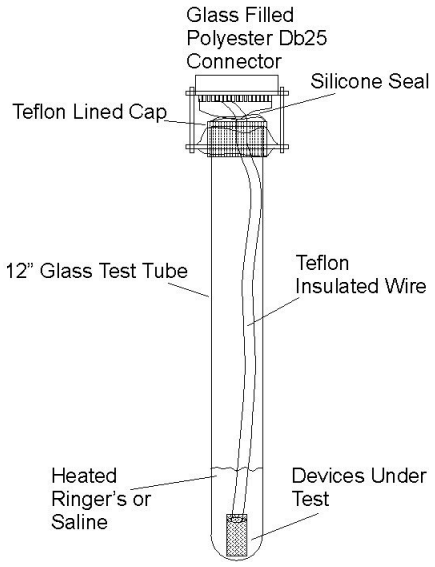

Fig. 4. Long tube test vessel. These are placed in heated aluminum blocks up to the level of the solution which is maintained at temperature ±1°C by a closed loop feedback controller. The upper portion of the tube stays near room temperature and acts as a reflux condenser.

Two heater blocks are in use at 37°C, and 90°C. Each heater block holds up to 32 test tubes, each of which contains four test devices (for a total of 128 devices per heater block). Every test tube has a standardized cable that connects it to a custom-built circuit board that biases its soak solution to a set voltage and measures the leakage currents of the four test devices it contains. The current-to-voltage conversion factors are $10^9\ \Omega$ and $10^{12}\ \Omega$, in order to measure equivalent resistances from $10^7\ \Omega$ to $10^{15}\ \Omega$.

An example of open circuit data from a set of 4 electrometers is shown in Fig. 5. In this particular case, a 3 ft long extension cable typical of those used to connect to older devices was left in place with no device plugged into it. From this data it is clear that while there is some noise associated with the measurements, it should be possible to reliably monitor resistance levels up to $10^{15}\ \Omega$ (Fig. 6). This data could also be smoothed considerably which would allow even more sensitive detection of trends.

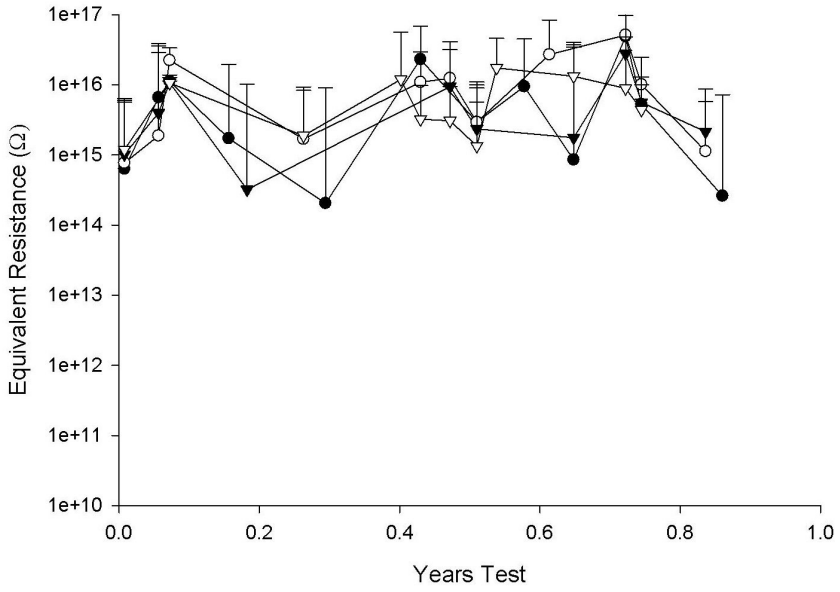

Fig. 5. Open circuit test of one set of four electrometers in the 384 channel system. Missing data points are caused by random fluctuations giving negative resistance readings which do not plot on log scale. Error bars are shown as positive only because of the log scale.

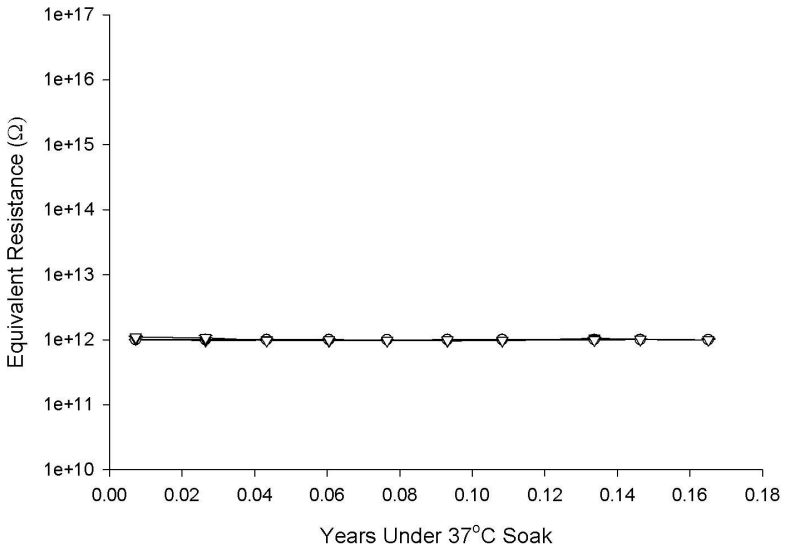

Fig. 6. Example of measurement of 10^{12} Ω calibration resistor set. One standard deviation error bars are too small to be visible.

3.2.2. In-vivo instrumentation

A portable 4 channel electrometer system was developed for monitoring devices implanted in animals. Initially, a relatively high bandwidth electrometer head stage was used to minimize settling time and artifacts. However, there were substantial problems with input protection, static electricity discharges from fur (particularly in winter), and the mass of the assembly relative to the fragile bone mounted connectors. In addition, it was necessary to wait at least 10 minutes between voltage steps to allow the devices being measured to settle. Because the settling time was so long anyway, the system was re-designed with the electrometers safely protected in a shielded box with 10^8 Ω input protection resistors and 0.1 μF low leakage capacitors across the $1x10^9$ Ω feedback resistors of the electrometers. This provided a 100 s time constant which effectively removed spurious signals and allowed use of an interconnecting cable between the amplifier box and the implanted connector. Ten minutes was sufficient for transients to decay after stepping the bias voltage for each measurement.

In order to maintain a constant voltage bias between measurements, a miniature 6 V battery pack that minimally increased the size of the implanted connector was developed with diode protection to limit current to the leakage of the diodes (~5 nA). A sketch of an assembly is shown in Fig. 7.

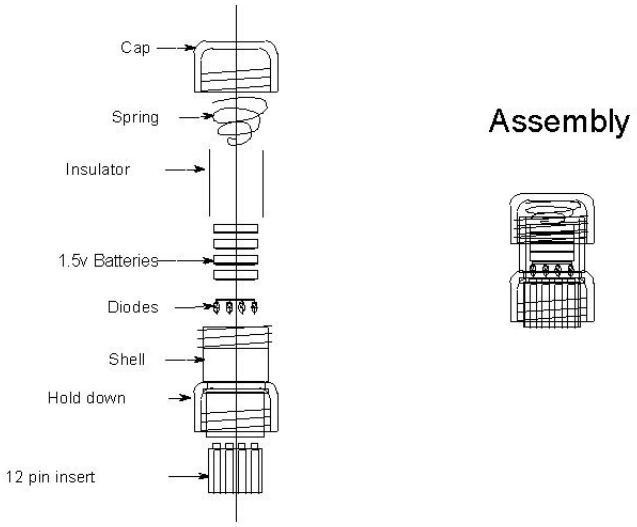

Fig. 7. Battery pack developed to provide continuous 5 V bias current limited to 0.1 μA.

In actual use, animals are only tested occasionally to minimize risk of damaging the connectors during the long measurement sequence. Measurements were reduced to two data points to maintain the overall animal restraint time to less than 30 min. Thus the accuracy of the system is severely compromised. Overall, this was a very cumbersome system that eventually was replaced with an implantable system that can make continuous, sensitive measurements without external connection.

3.2.3. Totally implantable measurement system with CMOS IC integrity monitors

A totally implantable measurement system was developed to eliminate connectors for a long term *in-vivo* measurement system for various implantable test devices. This system could also be used to evaluate CMOS integrated circuit integrity as well. An integrated circuit forms the heart of this system and is called the "PassChip". During work to develop a brain signal telemetry unit which was funded by the Department of Veterans Affairs[29], and insulating biomaterials implant work funded by NIH-NINDS[30], a low power, single channel optical transmitter system was developed. The implant received power by infrared transmission to implanted silicon photodiodes, and transmitted by light from an LED a single channel of EEG from implanted brain electrodes. This device was quite large and consumed much more power than would be available for the insulating biomaterials application, but the success of that device established the possibility of accomplishing the goal of developing a totally implantable multichannel electrometer data transmitter. Because LEDs require hundreds of microamperes of current for a robust signal, a Pulse Position Encoding (PPE) technique for power efficient, low noise transmission of neural signals was used to replace a percutaneous connector. PPE consists of converting a voltage to time between pulses. By minimizing pulse width, and utilizing high speed photodetection circuitry, it is possible to greatly reduce power consumed by the LED transmitter.

In order to design an integrated circuit version of a low power/low noise PPE encoder/transmitter, it was necessary to develop an understanding of noise/power tradeoffs in micro-power CMOS integrated circuit design[45]. The optimal designs required a minimum area for flicker noise, a minimum current for thermal noise, and a minimum gate width for operating at the knee of the sub-threshold region to maximize transconductance for a given bias current. This key understanding allows implementation of integrated circuits amplifiers, encoders and telemetry that operate with minimum power requirements while still meeting noise and bandwidth requirements.

A new, fully implantable measurement system was then developed. Since the device would be based on CMOS integrated circuit technology, it was essential to first monitor CMOS parameters and dielectrics to ensure that the measurement system would survive implantation. In addition to surface leakage current IDEs, other diagnostic sensors were included on the implantable test chip.

Silicon integrated circuits typically use a variety of dielectric layers. Some of these layers contain soluble materials such as boron and/or phosphorous that could lead to formation of low conductivity pathways and corrosion. MOS devices require low electrical leakage, charge stable dielectrics for many circuit applications. Intrusion of water and ions from the biological environment can cause increased electrical leakage through gate oxides and could also alter the fixed charge within the oxide. There are perhaps other long term failure modes as well that have yet to be discovered since there is little experience with embedding MOS integrated circuits within biological systems without benefit of hermetically sealed titanium canisters. The threshold voltages for Schmitt trigger voltage sensors were monitored by the channel marker interval which was inversely proportional to the Schmitt trigger threshold. Reversed biased diodes protected or unprotected by metal and unprotected monitor PN junction leakage currents for detection of water and ionic contamination of the silicon substrate were used. Test devices for monitoring the surface leakage currents of metal traces encapsulated with silicones or other appropriate materials were included. Bond pads for monitoring an external device allow for testing of wire insulation for example.

One major issue with an automated test system that could be implanted was how to best transduce the low level currents being measured into a useable readout. *In-vitro* testing utilizes expensive, large, high value resistors in current to voltage converting electrometers to provide sensitive readout of low level signals. However, since IC dielectrics are very good insulators, it may be that the leakage currents would be difficult to sense even with very high value resistors.

An alternative was to use a charge integrator with low leakage MOS integration capacitors as shown in Fig. 8. Charge from leakage current (I_{leak}) is integrated onto C_i of the input integrator continually. When the output of the on-chip integrator drops below Vref, C_i is reset to the "high" Schmitt trigger threshold by a high impedance switch. The output of the integrator is monitored by a readout capacitor which periodically samples the integrator output voltage onto a readout capacitor. The resulting charge packet is then removed by the readout current source I_o or I_m in the case of the marker channel. When the output capacitor voltage drops below Vref, the output Schmitt trigger turns on the output LED and resets the output capacitor voltage to the next voltage level to be transmitted. The time it takes to remove the charge from the readout capacitor is proportional to the on-chip integrator voltage. The decoder receives the light pulse and converts it to a voltage pulse which is used to reset the decoder integrator. The voltage that the decoder integrator attains prior to reset is proportional to the time between incoming light pulses and hence is proportional to the on-chip integrator voltage being transmitted.

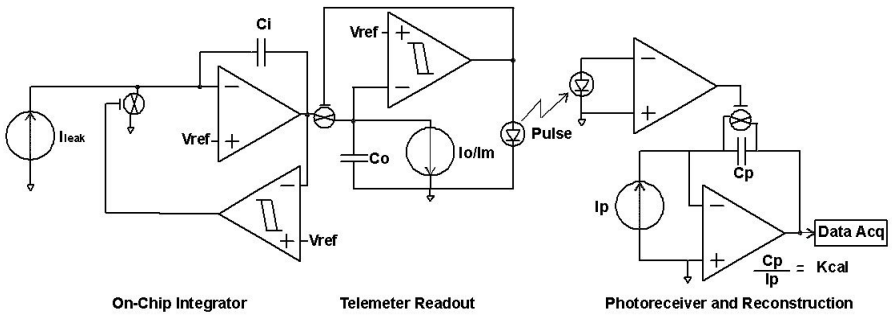

Fig.8. Functional diagram of PassChip implantable integrated circuit.

During a given measurement episode where the readout of the devices are recorded, if there is no detectable change in the output from a particular integrator, then that device may need to be monitored at daily or longer intervals to detect the leakage current. Thus the dynamic range of the system can be quite high. For example, with the average readout rate set at 100 Hz for the 14 channel device recently designed, each channel would be readout every 0.14 s. Thus if the fastest integrator reset occurred every 1 s, multiple

samples of the integration slope could still be obtained. By designing the integration capacitor to be 2 pF, the highest leakage current that could be easily monitored was be 5 V x 2 pF / 1s = 10^{-11} A. Higher leakage currents would begin to exhibit aliasing since the sample rate would be too low.

However, for the devices being considered here, leakage currents higher than 10^{-12} A would indicate significant device degradation. The lowest current that can be monitored with this design is limited by the parasitic leakages associated with the integration node, probably dominated by the reset switch (~$4x10^{-16}$ A). A $4x10^{-16}$ A leakage current would take approximately 50 s to cause a 10 mV shift in the output of the integrator. The noise level of the telemetry system was less than 10 mV, so this signal is easily detected, especially when using linear regression to compute the slope because of the inherent averaging effect. By monitoring for a few minutes then, it is possible to gather enough data to accurately measure the integration slope. While the leakage current associated with the reset switch could be minimized further by various guard techniques, it is useful to have a positive leakage current that will show that the integrator is functioning normally in the absence of leakage current from a device under test. By including an integrator that simply measures its own leakage current, the actual parasitic leakage currents can be estimated. Calibration is accomplished by including a miniature glass encapsulated, pre-calibrated 10^{12} Ω resistor as a test device on one channel. With this configuration, decoding and scaling is accomplished by taking the ratio of the slopes of each channel relative to the calibration channel, scaled by the calibration current or calibration resistance.

In all testing it is important to include a means of detecting whether or not the two interconnects to the device under test are indeed connected. If either of the interconnects failed, the device could be open circuited and could thus output erroneous very low leakage current readings. To detect this condition, the bias voltage connection to the device under test was used also as the power supply connection for the integrator/detector stage. The sensing connection to the integration node was also used as the reset interconnect. If either failed, the integrator output would fall to ground and would remain stable over time. This is an odd condition for the system because it implies that there is a very high input current to the integrator, but the integrator output does not change. Thus it is a unique fault condition that cannot be confused with a low leakage current condition. Channel marking was accomplished by sending the power supply voltage to the output stage. Since the individual integrators only reset the integrator output to the Schmitt Trigger threshold, the power supply output voltage is also unique and can be used to detect channel 1 for de-multiplexing the transmitted signal.

The overall implant scheme is shown in Fig. 9. The lithium batteries should last for over 9 years. It would be possible to replace the batteries in a short, minimally invasive surgery, though this should not be necessary during the life of one rabbit. Otherwise, the animal can be terminated, the device removed, cleaned, sterilized and re-implanted in a second rabbit for longer term testing. To guard against damage to the animal from a power lead or circuit fault, 10 kΩ series resistors with 0.1 μF bypass capacitors were connected to the battery anode.

Readout of the implants requires no restraint of the animal. Simply by holding the photodetector close over the LED will pick up the relatively high intensity though brief flashes from the transmitter. The acquired pulse train is then de-multiplexed and decoded using analog circuitry. The reconstructed signals are acquired by a portable data acquisition computer and the leakage currents computed and archived.

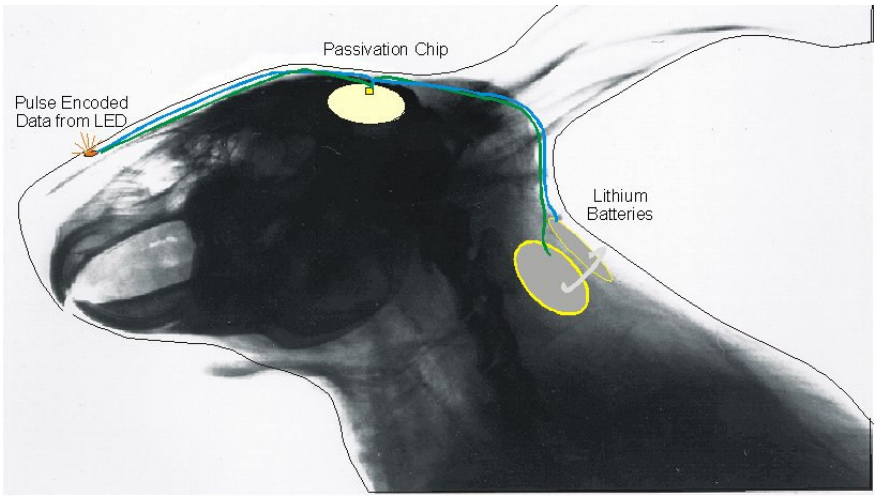

Fig. 9. Sketch overlayed on x-ray of rabbit showing locations for components of totally implanted PassChip sensor telemetry system.

Several test circuits for these concepts were designed, submitted to MOSIS for fabrication, and evaluated. There were five circuit related bond pads for connecting an external bias setting resistor, power supply, the LED output, and reset for initializing the shift register after power up. Pads for an external device were included to allow attachment of wire loops or some other external test device such as a calibration resistor. They could also be connected with short wire loops to test bond pad leakage currents directly. The central corridor of the chip contains a loop of low power shift registers that continually cycle through the integrators to function as a channel sequencer. Double rows of integrators are located on either side of the shift registers. The test devices are connected to the integrators. The outputs of the integrators are bussed to the readout stage. The readout sequence consists of setting the capacitor to the integrator output voltage using a p-channel source follower on the output of the integrator being addressed, and then pulling off the signal charge using a constant current source until an arbitrary threshold is crossed which generates a pulse from the LED transmitter which causes the circuit to shift to the next channel and repeat the sequence.

There were 14 channels included on this implementation. One channel was used as a marker for identifying Channel 1. Another channel was used to measure the open circuit leakage current of an integrator stage. Two channels were used to monitor the reverse biased leakage current of 3600 μm^2 diodes. One of the diodes was shielded with Metal 2 and the other was not. Another channel was used for monitoring the external device bond pads. The remaining nine devices were used for on-chip test structures. The on-chip test structures were of two varieties. One was an array of conductive fingers overlaying a second array of conductive fingers with the dielectric to be tested in between. These can be thought of as vertical testers and are designed to detect failure of the dielectric between two layers.

An example of a vertical tester is shown in Fig. 10. This structure consists of an array of lines of polysilicon on two layers separated by a thin silicon dioxide dielectric. The integrator will acquire electrons that flow from one polysilicon layer to the other through the thin dielectric. The active area is large and there are 2 µm wide slots between every finger thereby ensuring that the device will be sensitive to water and ionic contamination. Vertical test devices included Metal 1 – Metal 2, Polysilicon 1 – N-Well, Metal 1 – Polysilicon 1, Metal 1 to Polysilicon 2, and Metal 2 –Encapsulant. The Metal 2 – Encapsulant device was to measure the bulk resistivity of whatever encapsulant was used to protect the outer surface of the chip.

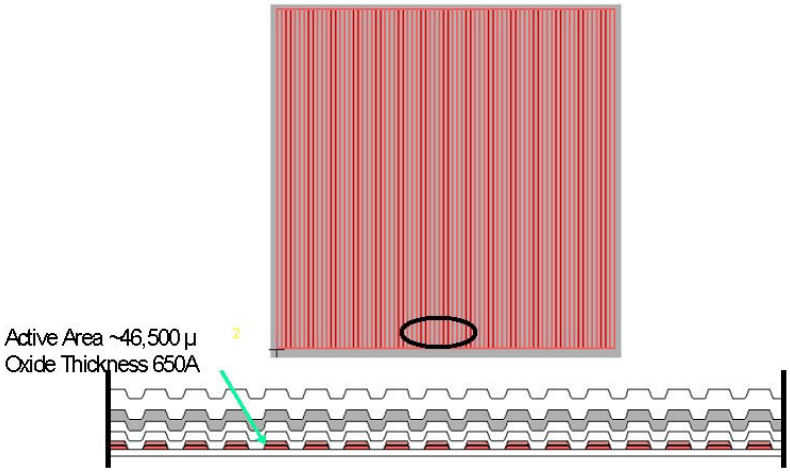

Fig. 10. Example of vertical test structure shielded by Metal 2 (solid grey squiggle). Arrow points to one line of this multi-line structure with polysilicon 1 and polysilicon 2 separated by a thin silicon dioxide layer.

A second type of on-chip test device was the Interdigitated Electrodes (IDEs) which tests the integrity of a particular dielectric layer and interface. An example IDE testing the Metal 1 layer is shown in Fig. 11. Because of the relatively small features and large test area, there are about 10^4 squares (sq) for leakage current to flow. If the ultimate sensitivity of the measurement was be approximately $5x10^{-16}$ A for a 5 V bias, the effective surface resistivity that can be sensed would be approximately 10^{20} Ω/sq which should provide early indication of potential faults with MOS circuit protection in biological systems.

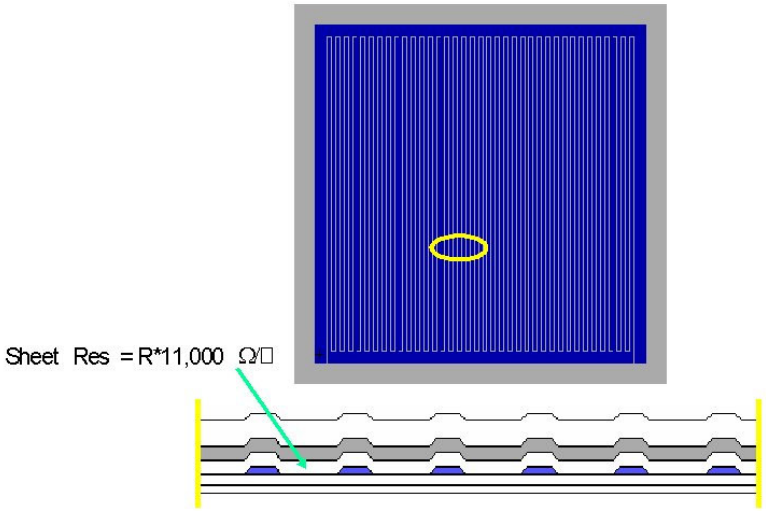

Fig. 11. Interdigitated electrode array (IDE) for MOSIS 2µm n-well process. IDE is formed with Metal 1 while Metal 2 and the outer passivation layer provides additional protection.

3.2.4. Summary of PassChip

In sum the PassChip has the following characteristics:

- Vertical grids check dielectric conductivity;
- Interdigitated electrode arrays for lateral resistivity;
- MOS threshold monitors;
- Power and bias monitors;
- External test device connections;
- Implantable in CNS with transcutaneous transmitter;
- Lithium TC batteries supply 4 µA for >9 years;
- Ultra-low power encode/mux/transmit circuit (~3 µA);
- High sensitivity, continuous calibration.

An example of the output pulse train and decoder integrator output is shown in Fig. 12. The wide pulse interval is the marker channel. The subsequent intervals are channels 1-14. Signal reconstruction occurs by sampling and holding the decoder integrator voltage at the time of the decoder integrator reset caused by the arrival of the interval ending pulse.

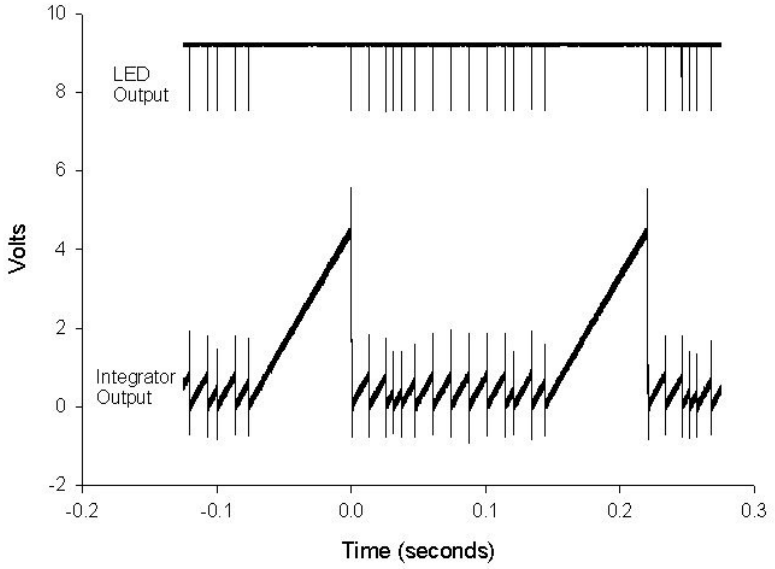

Fig. 12. Output pulse train from PassChip (LED OUTPUT) and decoder integrator output.

3.3. Assembly of PassChip for implantation

Due to the high impedance input structure, the PassChips were particularly prone to damage by static charge buildup resulting in ESD (electrostatic discharge). Figure 13 LEFT shows a PassChip that was damaged during pre-cleaning by ESD. Since rendering the lab ESD safe, successful assemblies are relatively routine.

LED modules were hand assembled in a "free-wire" topology to maximize sealing around devices by silicones (Fig. 14 LEFT). Future assemblies will use alumina hybrid circuit substrates and a solder-reflow process for greater strength and reliability. Figure 14 RIGHT shows a completed PassChip implant assembly soaking in sterile saline prior to implantation. The LED module is attached to the PassChip with three fine Teflon® coated wires that are over coated with silicone. The LED module is also attached to the power supply with two Teflon® coated wires strain relieved by a silicone impregnated fiberglass ribbon.

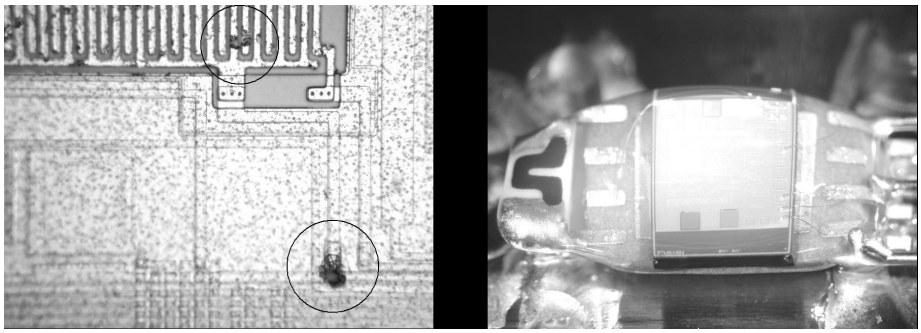

Fig. 13. LEFT: Micrograph (Interdigitated electrode width/space = 2 µm) upper circle showing ESD damage causing bridge between traces. Lower circle highlights crater formed from ESD damage between a power supply trace and the shield. Damage occurred during pre-assembly cleaning procedure. RIGHT: Encapsulated PassChip sub-dural implant portion showing carrier with PassChip attached in center and bonded to calibration resistor on left (Ω marking) and output leads on right.

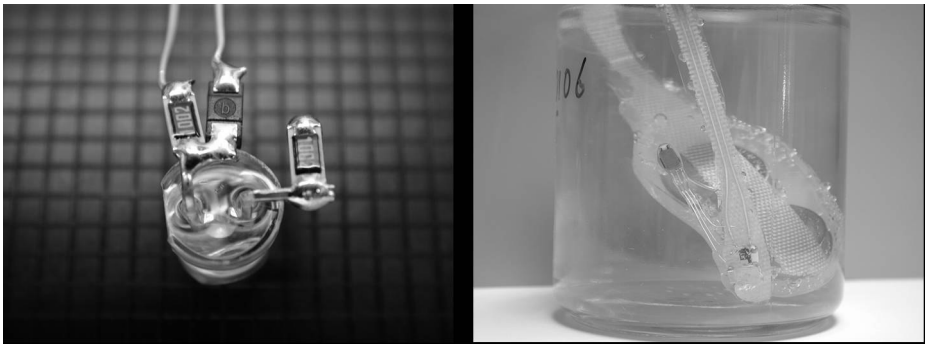

Fig. 14. LEFT: LED module shown from underneath. Resistor/capacitor network limits current during a pulse and also decouples the power to the LED from the PassChip to minimize power supply cross-talk. RIGHT: Completed assembly in sterile saline soak prior to implantation. LED module is near bottom, front/center of jar. Backside of sub-dural PassChip is visible near center of picture attached to LED module by fine Teflon® coated wires that have been encapsulated in silicone. Twin lead reinforced with fiberglass and silicone connects to battery pack.

3.4. PassChip Implant Results

Fig. 15 shows a 3 week post-op rabbit with LED functioning continually. The photograph was taken in low light with a 1/10 s shutter speed to collect ten LED flashes. Data is normally taken by placing a high speed photodector over the skin and fur covering the LED.

Fig. 15. Rabbit with implant 3 weeks post-op. Bright spot is LED taken in low light with high sensitivity camera setting.

Example X-rays of an implanted PassChip are shown in Figs. 16 and 17. The battery pack is relatively bulky and was placed between the shoulder blades in a subcutaneous pocket. Power supply leads were tunneled under the superficial muscles of the neck to minimize flexing of the leads. The actual PassChip is implanted in contact with the pia, completely under the dura. For a period of at least 3 months, the dura does not grow down and around the implant but instead seals to the silicone encapsulated leads that exit the skull. This may not be the outcome for very long term implants.

An example of raw data taken from one channel of one implant after several weeks *in-vivo* is shown in Fig. 18. This implant included a calibration resistor on the terminals of the external test device. The calibration resistor was 0.96 TΩ ($0.96 \cdot 10^{12}$ Ω) and was biased at 2.35 V relative to the input to the integrator to generate a 2.35 pA calibration current. The 0.96 TΩ resistor was a thick film glass encapsulated device that should remain relatively constant over time. With the calibration signal from the implant, conversion of the other channels of data simply consists of scaling the calibration current by the ratio of the readout channel to the calibration channel slopes. This is a much more accurate method of calibrating the implants that has the huge advantage of being only dependent on the true magnitude of the calibration current. All of the other circuit drifts are nulled by the ratio including threshold voltage drifts unless they occur in isolated parts of the circuit. Temperature drift is completely nulled as is power supply drift. The striped appearance of the raw data is caused by quantization of the signal into increments of 4.88 mV by the 12 bit A/D converter used to gather this data. Because the data is effectively averaged by the linear regression process, this quantization effect adds little true noise to the system. Moving to 16 bit A/D conversion would reduce this effect by a factor of 16. The current noise was computed from the standard error of the regression fit and is quite low due to the averaging effect of the encoding and decoding integration processes and the linear regression fit. Other channels exhibit similar characteristics and accuracy.

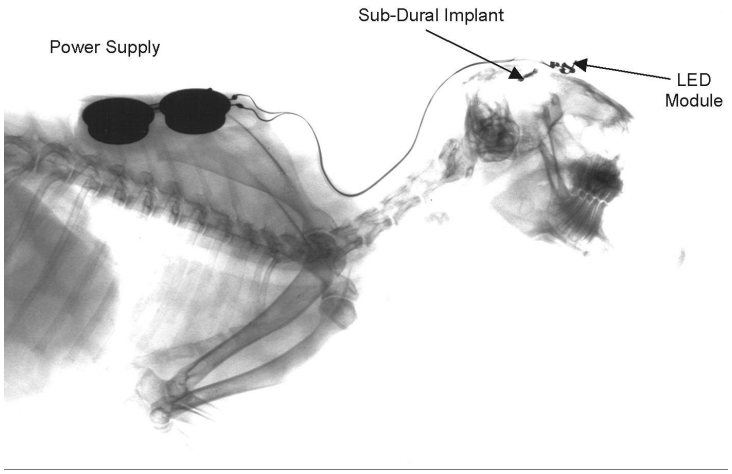

Fig. 16. Lateral X-radiograph of PassChip assembly implanted in rabbit. Power supply, twin-lead interconnect, PassChip (labeled sub-dural implant), and LED module are visible. Power supply leads were tunneled under the superficial muscles of the neck to minimize flexing.

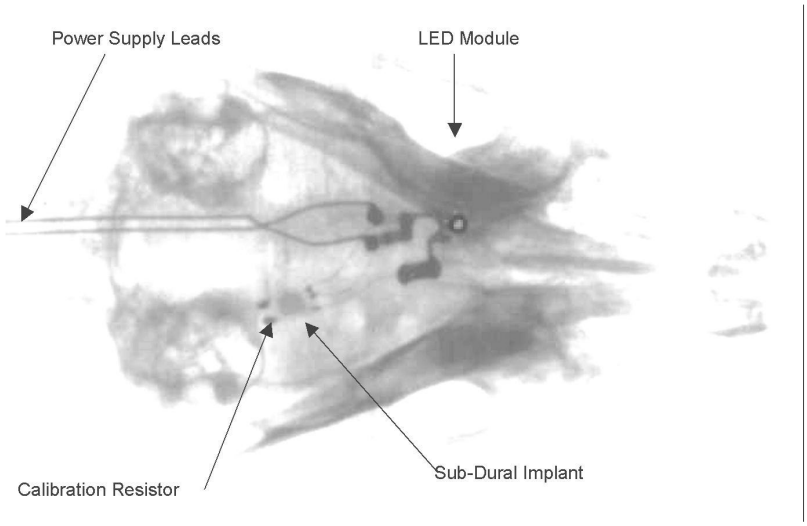

Fig. 17. Example X-radiograph of sub-dural implant showing the power supply leads, PassChip (labeled sub-dural implant), calibration resistor and LED module.

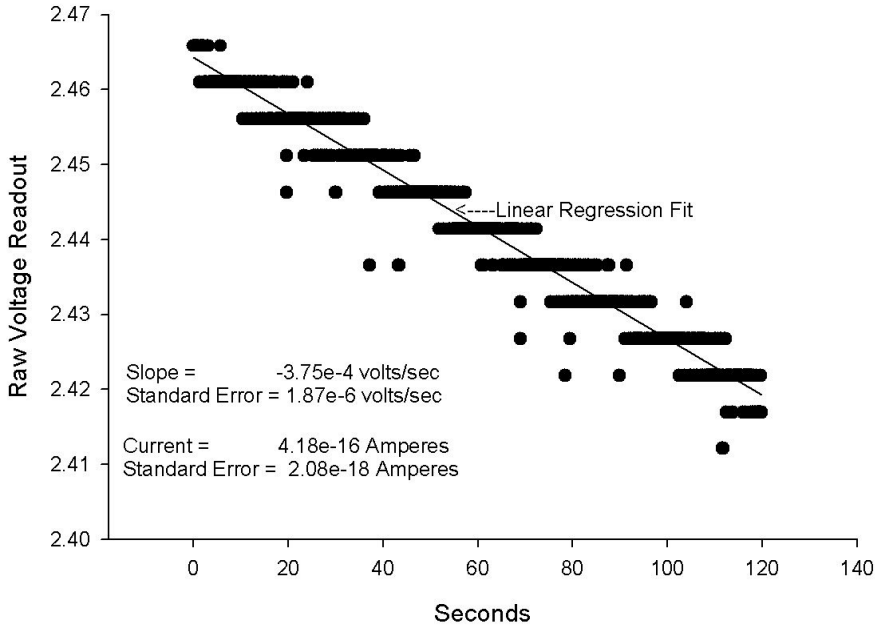

Fig. 18. Example of raw data taken from PassChip open circuit integrator (channel 14) several weeks after sub-dural implantation in awake, unrestrained rabbit.

Data from one implant is summarized in Fig. 19. Note the stability of the marker channel indicating the stability of the power supply. Most of the devices behaved as expected. The diodes showed negative changes but this was due to the data being taken in the dark versus the intense illumination from surgical lighting. Metal 2 IDE also showed a negative change in leakage current (leakage current reduced during soaking). This might be due to anodic oxidation of one half of the alumina traces of the IDE, oxidation of a contaminant, or improved bonding of the silicone interface as is often observed with silicones. All of the other devices exhibit increases in current with the Gate on N-well waffle pattern (Channel 6) showing the largest increase. It may be that there is infiltration of water molecules into the gate structure, but it seems unlikely over such a short time interval in view of the results of other sensors on the same chip. It is also possible that this sensor was more affected by light during the initial readings, perhaps due to photon aided electron transport through the gate oxide.

In summary, the new, improved strain relieved implants will be placed this spring. The two functioning implants will be allowed to continue as long as they can at least be intermittently reset to demonstrate that the CMOS circuitry is still operational and that the power supply is intact.

Chan	Device	9/19/01 Light	10/5/01 Dark	% Increase	Units
1	Marker Voltage (Power Supply)	6.92E+00	6.92E+00	0	Volts
5	Diode	1.10E-14	9.95E-15	-10	Amps
4	Diode near M2 shield edge	1.26E-14	7.65E-15	-40	Amps
7	M2 IDE bare on surface	1.13E-12	7.15E-14	-94	Amps
6	Gate on N-well Waffle	2.93E-16	1.58E-15	438	Amps
13	M1-P2 w/M2 shield	6.86E-16	1.44E-15	111	Amps
9	P1 IDE w/M2 shield	3.70E-16	6.04E-16	63	Amps
2	M1 IDE w/M2Shield	8.06E-16	1.19E-15	48	Amps
3	M1-M2Waffle w/Poly+M2	6.29E-16	8.70E-16	38	Amps

8	P2 IDE w/M2 shield	9.81E-16	1.26E-15	28	Amps
14	Open Circuit Integrator	6.80E-16	8.19E-16	20	Amps
11	M2-out Large Pad	8.64E-16	1.02E-15	18	Amps
10	P1-P2 Waffle w/M2 shield	6.95E-16	7.12E-16	2	Amps
12	Calibration Resistor	2.45E-12	2.45E-12	0	Amps
Cal	Cal Resistor (ohms) @2.35v,	9.59E+11	9.59E+11	0	Ohms

Fig. 19. Initial post-op readings taken in operating room with surgical lights on and readings taken in animal dark animal cage a few weeks later. The diodes show negative increases because of the absence of light. The M2 IDE under the silicone encapsulation also shows negative change.

The functional assemblies were implanted as two groups, 3 in the first group and 2 in the second group. In the first group, all devices functioned normally during pre-implantation soak and post-implantation measurements. However, all three power supplies were exhausted after several weeks. The cause of the power supply failures was the two conductor ribbon cable interconnect between the batteries and the LED/subdural implant. The ribbon cable was a multi-strand silver plated copper conductor with FEP insulation. The FEP apparently had been laminated rather than extruded, and during the final cure it de-laminated in places along the 6 in. length. Eventually, moisture collected within the de-laminated segments causing a low impedance path between the power supply leads which discharged the batteries.

Attempts were made to replace the power supplies with new modules and wiring. While it was possible to temporarily repair one unit, the repair itself failed after a few days due to the difficulty of re-encapsulating the connections *in-vivo.* The two other devices had other faults as well. One device had a broken micro-lead that runs from the LED to the PassChip itself which may have been caused during removal. The encapsulation on another PassChip was thinned near the edge of the PassChip itself and this region split, exposing the bottom edge of the silicon chip. This was probably caused during implantation as the device was slipped under the dura. The third device was apparently intact, but did not recover when re-connected to a new power supply. This could have been caused by static damage during inspection, or by loosening of a wire bond during all of the handling.

In all three cases, however, the bond area and surface of the PassChips showed no degradation as may be seen in Fig. 20. Also shown in Fig. 20 is the double bonding technique afforded by use of 0.7 mil gold bonding wire. This photo was taken through the silicone encapsulation. The rings around the bond pads are shield isolation rings. Higher magnification of the bond-pad interface showed no corrosion of the aluminum/gold interface in spite of high temperatures used in curing the silicone and several months in saline and implanted.

Fig. 20. Explanted PassChip after several months in-vivo exhibiting no corrosion or other visible changes to the device surface. Photo taken through silicone encapsulation. Dual bonds were for reliability. Diameter of single gold wire lead visible on right side of chip was 0.7 mil.

The second group was fabricated with PFA insulated multistrand wire. The power supply wires were individual, and were further encapsulated in silicone. Encapsulation of the PassChip was more uniform and thicker over critical sharp edges. These devices functioned well before and during implantation. However, after several weeks both devices began exhibiting intermittent behavior. The devices are still functioning, but intermittently. Thus, it is not possible to obtain data that can be interpreted in terms of the leakage currents. Still, for the CMOS system to be able to telemeter a pulse train, relatively complicated, high impedance, low current mixed analog-digital circuit is operating correctly. The problem with these two devices is the relatively rigid interconnect between batteries and implant that is apparently causing excessive stress on the silicone skull plug and strain relief sutures. The fine wires that connect the LED and power directly to the chip holder are multi-strand silver micro-wire but they cannot withstand constant flexing within silicone encapsulant.

The third generation implants will have a smaller wire interconnect between the battery and LED module that is strain relieved with the silicone fiberglass developed for this purpose. There will be a small stainless steel plate pre-drilled with two mounting holes for fixation to the skull. The LED module will also be mounted on this stainless steel plate. Once that is in place, the fine wire interconnects to the sub-dural PassChip will be strain free. Another improvement will be to use hybrid circuit assemblies for producing the power supply regulators and the LED module that will greatly improve the mechanical stability of the assembly.

4. Materials and evaluations

Years ago, parylene and polyimides were viewed as the most likely materials to succeed as insulating biomaterials. However, since very little information existed on which to base such assumptions, a wide variety of materials was considered and placed under test. All of the major insulators known to be relatively inert chemically were screened. Only silicones, polyesterimide and Teflon® exhibited sufficient longevity to warrant continued testing.

There are two classes of materials proposed as the most promising insulating biomaterials in this project at present - fluorocarbons and silicones. Both of these films have been outstanding in a variety of tests. Many variations in chemistries are available, each with slightly different characteristics which allows

for developing a thorough understanding of the materials and how to apply them optimally. This conclusion is the result of testing a wide variety of materials in the past years.

This conclusion is not restrictive, but rather serves to focus the work on a reasonable number of alternatives. Other materials now being tested in limited experiments include parylene and polyesterimide. Parylene performs quite well for short term implants. In clinical applications, for short term implants or animal studies, required resistances are much lower than those routinely used to test insulating biomaterials. Rigorous testing of Parylene has yet to produce results similar to those observed for fluoropolymers or silicones. In view of reports by others indicating hydrolytic weakening and craze cracking of parylene under high humidity conditions[46], it seems unlikely that parylene in present form will prove stable for long term implantation.

Polyesterimide shows considerable promise as a wire coating where the concentric nature of the coating renders the adhesion issues irrelevant. Polyesterimides have withstood over 5 years of saline immersion without failure. While not as good an insulator as Teflon®, polyesterimides can be applied to much finer wire diameters than Teflon® and thus may still find an application.

Polyurethanes have also been tested and have shown that there is a slow but steady increase in leakage current over time. The extrapolated lifetime base on these measurements was on the order of 20-30 years. Polyurethanes have been extensively studied by those interested in cardiac pacing lead technology. While originally thought to be an improvement to silicone elastomer coated leads, polyurethanes were not thoroughly tested prior to being used for pacing leads. Subsequent studies revealed that polyurethane is severely attacked by the biological environment causing loss of mechanical properties, cracking, and loss of insulative properties [15,40,57]. The history of the use of polyurethane in biological systems teaches that *in-vivo* testing must be done with due consideration of the final application *prior* to introduction of a new material.

Thus it seems reasonable to continue exploring the versatile, high performance coatings that have already been identified as highly successful insulating biomaterials - silicones and fluoropolymers. Other materials such as Kapton/polyimides, epoxies, and new materials will continue to be evaluated *in-vitro* to define the limits of these very useful but relatively short lived insulating biomaterials.

4.1. Use of silicones as an implantable material

Silicones are by far the most studied of all classes of biomaterials. Commonly used as breast implants, penile implants, testicular implants, joint replacements, cerebrovascular shunts, heart valves, cardiac pacing lead insulation, indwelling catheter material, intraocular lenses, carriers for cochlear electrodes, etc., silicones are the most biocompatible, long lasting material yet developed. Currently, silicone breast implants are still considered reliable and safe by the American Society of Plastic Surgery[11]. The main problem with older implants appears to be contracture of the fibrous capsule causing extrusion of silicone gel and oil into the surrounding tissue. Gels and oils cause intense biological responses and can lead to generalized immunologic responses[39]. Current investigations indicate that it may be possible to prevent the typical fibrous encapsulation of silicone implants by coating the silicone with a hydrophilic layer of collagen or povidine[9,60]. In a study of cochlear implant electrodes [56,58], silicones showed no evidence of degradation following implantation for 16 weeks in the scala tympani and muscles of cats. This finding may be particularly important since the cochlear fluids are similar to cerebrospinal fluids. Also, there was only a mild reaction to the silicone resulting in a tight fibrous sheath which is commonly found with this material. Mechanical tests of implanted silicones have also been conducted in humans [12,16].

Heart valve poppets (balls of silicone) implanted for 52 days in a human had a surface to core dynamic shear modulus ratio of 0.98 meaning the outer surface of the balls had become slightly softer than the inner core. After 8 years, the ratio was 0.83 indicating progressive softening of the silicone material. They found that diffusion of water occurred faster than the degradation process. Perhaps other biomolecules were responsible for the mechanical changes.

The mechanical properties of the silicone insulation from pacemaker leads recovered at times ranging from 3 days to 11 years were studied [16]. Results showed that silicone tubing suffers gradual structural changes that are reflected in tests of swelling due to solvents (cross link density), and pull tests using the tensile strength at 200% elongation as a measure. Roggendorf et al.[52] tested a variety of materials including RTV silicones, a medical grade silicone, polyamide, and polyester. Implants were left for one year in dogs prior to analysis. In general for silicones, tensile strength decreased, elongation increased, and

the materials softened. Polyamide and polyester became brittle and exhibited crack crazing. They found that the stress-strain characteristic of the materials rather than hardness was the most sensitive to changes in mechanical properties. By Infrared Spectroscopy using Attenuated Total Reflectance, Roggendorf et al.[52] also showed that silicones took up lipid materials which may be related to the changes in mechanical properties. Roggendorf et al.[52] summarized their findings by stating that "If 'aging' is taken to include any irreversible change in a polymer after its manufacture, not one stable plastic or elastomer thoroughly tested under *in-vivo* conditions is known at this time.'' They go on to cite work showing that even Teflon®-PTFE becomes somewhat more brittle following implantation.

Pioneering work by PEK Donaldson [2,17-27] presumably motivated in part by his work on development of neuroprostheses in collaboration with G. Brindley [5,6] illustrated a number of issues involving the use of various types of silicone encapsulants for construction of long term implantable electronics. In spite of the permeability of silicones to water vapor, Donaldson demonstrated convincingly that silicones were remarkably efficient at protection of a variety of long term implants. Key aspects to the success of silicones were that substrates were metal oxides, surfaces were free of ionic contaminants that could drive osmotic formation of condensed water at the interface, and that the more negative surfaces were, the more effective silicones appeared to function.

This literature increases interest in testing the electrical properties of silicones, and comparing the mechanical degradation to electrical degradation. It also points out the need to be aggressive in testing with a variety of techniques to increase the probability that potential failure mechanisms are discovered.

Other aspects of the implant studies focus on the immune response and bacterial infection problem. The behavior of polyurethane, polyether/polyester copolymer, polypropylene oxide, and Silastic® tympanic membranes with Staphylococcus-aureus middle ear infections was studied[3]. Results showed that only the Silastic® implants were not degraded by the infection. Further, the fibrous capsule about the Silastic® was also not changed by the infection, and only rarely were macrophages observed between the capsule and the Silastic®.

Breast implant data, and studies of immune reactions to silicone indicate that under some circumstances, adverse reactions to silicone implants do occur, particularly when silicone oils or gels, or small fragments of silicones erode from implants[4,35,37]. Hunt et al.[42] in a study of liver pathology caused by circulating silicone particulates from kidney dialysis tubing were able to clearly identify silicone particulates in giant cells and verified the composition by X-ray Energy Dispersive Spectroscopy. This is a useful tool in the to check for erosion of the implants. Adverse tissue reactions to silicones are relatively uncommon experiences compared to the number of implants that show no adverse reactions. Should such reactions occur, they may involve the implant in a chronic inflammatory response which could significantly alter the environment that the implant is in. Evidence of infection or inflammatory response should be identified during *in-vivo* testing since an altered chemical environment may radically alter the outcome of the long term testing.

A special science panel appointed by the judge in the Dow Corning silicone litigations reviewed and critiqued the scientific literature relevant to the possibility of a "causal association between silicone breast implants and connective tissue diseases, related signs and symptoms, and immune system dysfunction."[14]. After reviewing over 2,000 documents presented by the legal counsels and through their own literature searches, the panel found no scientific evidence that silicone breast implants cause disease. In view of the very large mass and surface area of silicone implants compared to the very small mass and surface area of implantable micromachined devices, it is very unlikely that the implants for neuroprostheses will ever cause adverse systemic responses of any type.

4.1.1. Silicone encapsulation long term testing - 37°C saline soak

Figure 21 shows summarized results from a BondChip test. BondChips have four concentric rings of interdigitated electrodes. There are five pairs of electrodes in each ring, with 10 µm platinum traces separated by 20 µm spaces. Adjacent sets of electrodes are spaced 20 µm apart. Bonds are made in the center of the concentric arrays. The outer traces are within about 100 µm of the edge of the chip. These resistance measurements should be multiplied by approximately 4,000 to convert to ohms/square. The encapsulation material was Dow Corning MDX-4-4210. For the example shown in Fig. 21, the inner trace set failed after about 18 months. This could have been for several reasons, but the most likely is that there

was subtle contamination from the bonding process that shedded particulates on the inner traces that eventually created a conducting path. In spite of what must now be a fairly intense electrochemical environment within the failed traces, the adjacent traces have remained intact for more than 13 years thus far. This is a frequent but not totally consistent result for several silicone elastomers currently under test.

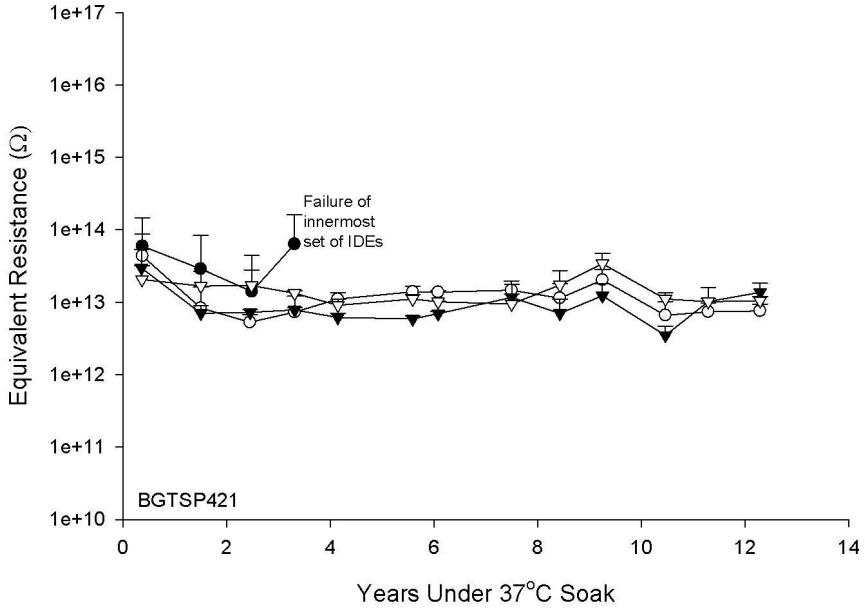

Fig. 21. Example data set from compiled results of long term soak testing with older single channel system based on the Keithley 617 electrometer, and the new 384 channel system based on discrete electrometer op-amps. The new system was used at the beginning of year 7 for BGTSP421, a silicon micro-technology based array of four concentric IDEs encapsulated with Dow Corning MDX-4-4210. Equivalent sheet resistance would be approximately 1e4 times these raw resistance readings. Data was non-uniformly sampled during one year averaging time periods. Error bars are shown as positive only due to log scale and are 1 standard deviation as computed from the actual variance of data within each period. Early failure of the innermost IDE was perhaps due to local contamination from wire bonding to adjacent pads.

Figure 22 shows results from a carbon filled experimental silicone (x6863C) obtained from Dow Corning electronics products division. This material is not available commercially. Initial readings were very high until soak testing began. One middle IDE began to fail after about 6 months. The outer IDE failed after 9 years while a more inside middle IDE failed after 10 years. While these results could have been due to inadvertent surface contamination of the sample or failure of the bulk properties of the material, it is more likely due to the carbon filler which provides isolated conducting paths throughout the material and particularly at the silicon dioxide interface. These isolated conductive paths could also serve to increase local field strength and perhaps cause focal dielectric breakdown.

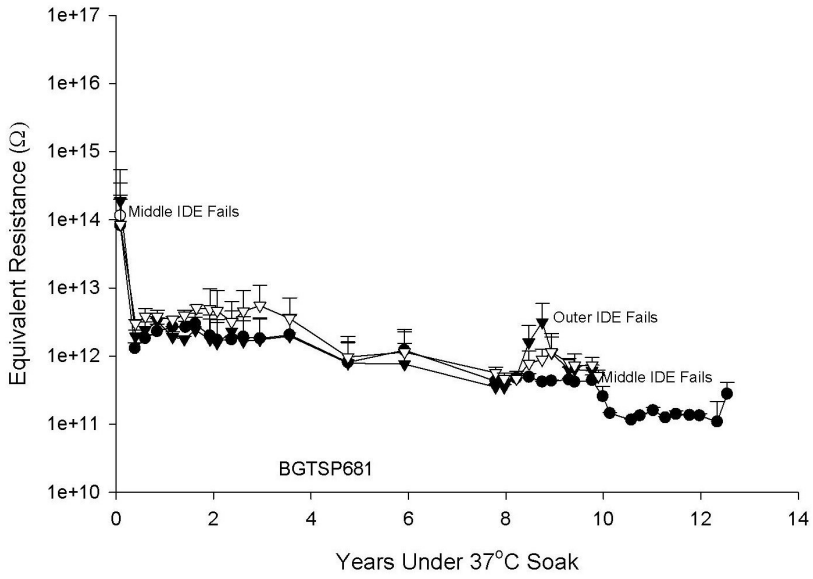

Fig. 22. Carbon filled experimental silicone (for light opacity) from Dow Corning (x6863C) on BondChip. Data averaged over 4 month intervals. Error bars are 1 standard deviation and shown as positive only.

Figure 23 shows long term soak results of a BondChip protected with x6863B without the carbon filler. This is a much better behaved sample where all four electrode sets have maintained high resistance readings for over 12 years. This plot shows perhaps some curvature but the readings between years 3 and 7 were too infrequent to have confidence in identifying a weak trend. However, data since 7.5 years has been taken on a weekly basis with the new electrometer system.

Figure 24 shows results from a BondChip with a similar material to x6863B but without an adhesion promoter (x8069). Contrary to expectations, this material maintained a higher resistivity than the x6863 (carbon filled or non-carbon filled) from the beginning and is continuing to demonstrate extraordinarily high resistance readings that are at the upper limit of the range of the new electrometer system. The Middle-Outer IDE set failed after about 2 years. In spite of this failure, the electrode sets on either side of the failed set continued to maintain very high resistance readings until recently when it appears that the Outer IDE set failed.

There are other examples of silicones, mostly successful, that may be useful for encapsulation of silicon dioxide surfaces. The only silicone materials that have consistently failed testing were resin filled systems. Resin fillers are used where optical clarity is important but mechanical strength is not an issue such as in the production of implantable artificial lenses.

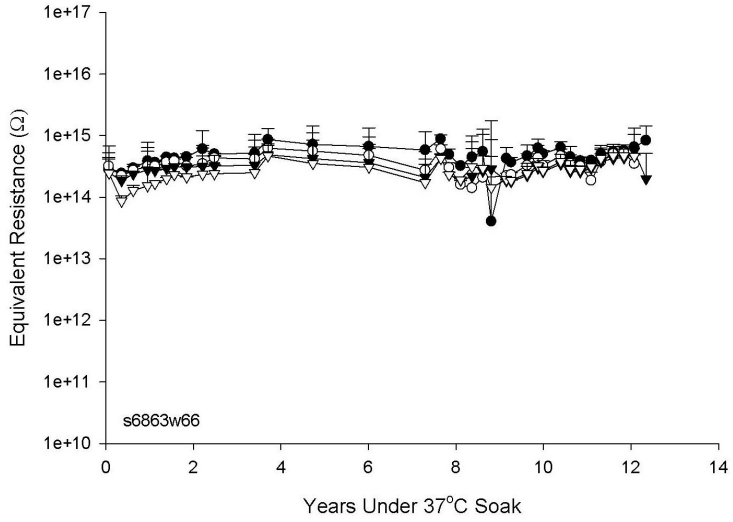

Fig. 23. Dow Corning x6863B without carbon on BondChip.

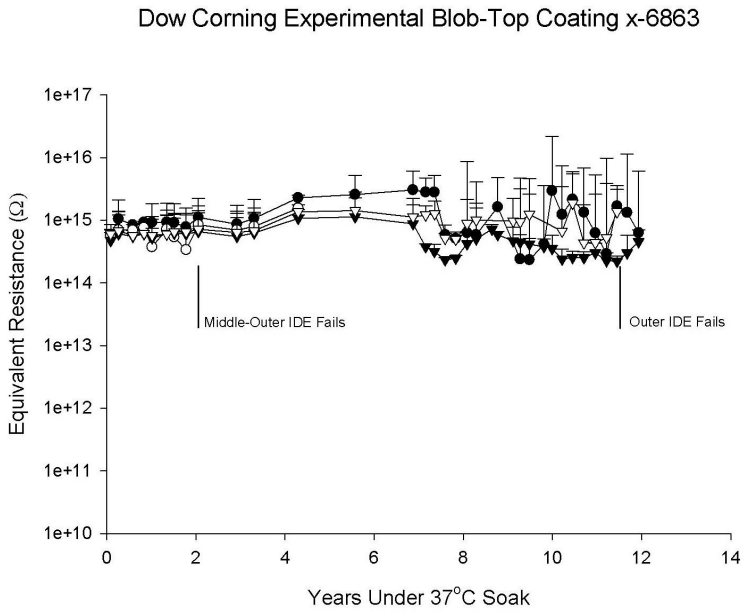

Fig. 24. Dow Corning x8069 experimental silicone on BondChip. Of the four concentric IDEs, the Middle-Outer IDE failed after 2 years, and then the Outer IDE failed after 11 years. The inner IDEs are still functioning well and are still under test.

4.1.2. "High" temperature saline soak

Triple track devices were developed to allow testing of the surface properties of the encapsulants without the confounding problem of particulates falling onto the test areas during bonding as was the case for BondChips. These devices have a single current emitting trace surrounded by two current sensing traces. Only one test device is included on each substrate, and four substrates are assembled into each test tube assembly.

Figure 25 shows results from long term surface passivation testing of CF20-2186 from Nusil on a triple track device. This is one of a few devices that so far have survived long term 90^{O}C saline soak. These devices are usually measured at 90^{O}C which adds additional noise to the measurement as well as reducing the resistivity. Due to lack of space in the high temperature system, this sample was moved to a lower temperature soak bath.

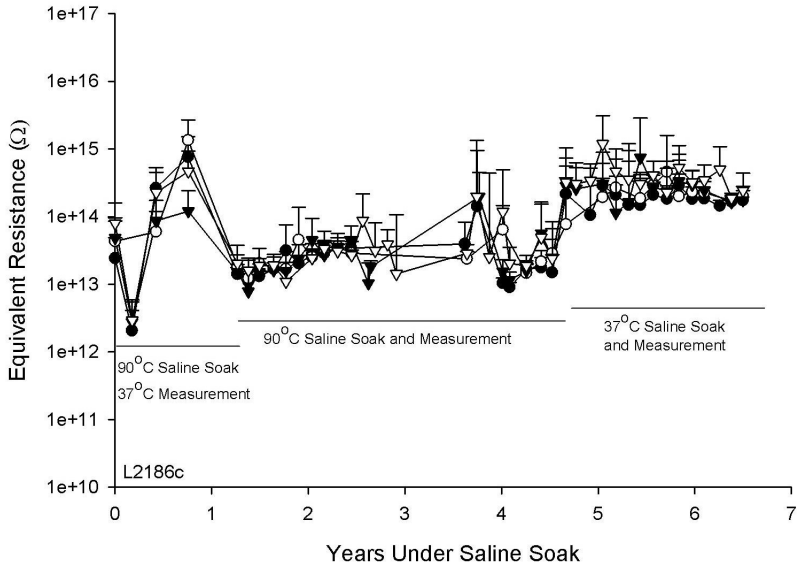

Fig. 25. 90°C saline soak test of Nusil CF20-2186 on 4 IDEs. Initially these devices were cooled to 37°C for measurements. Near year 5 the devices were left in a system that was changed to 37°C to make room for more samples, but will be returned to 90°C when an expanded system is implemented. Note that the lower resistivity measurements at 90°C compared to those taken at 37°C are due to the temperature dependence of the leakage currents.

A similar material from Hüls, Inc. (PEM25) has been performing well for over 9 years under 37^{O}C saline soak as shown in Fig. 26. However, as shown in Fig. 27, when soaked at 90^{O}C, the same material fails after about 3 years. If an activation energy of 1eV and first order chemical reaction kinetics is assumed as was used to construct Fig. 2, then a 3 year survival at 90^{O}C would indicate a 37^{O}C lifetime of about 700 years. Figure 26 summarizes data from the first 9 years of a 700 year test of this theoretical estimate. It is noteworthy that the variability of the devices shown in Fig. 26 is quite small once the automated system was implemented during year 4 of this test.

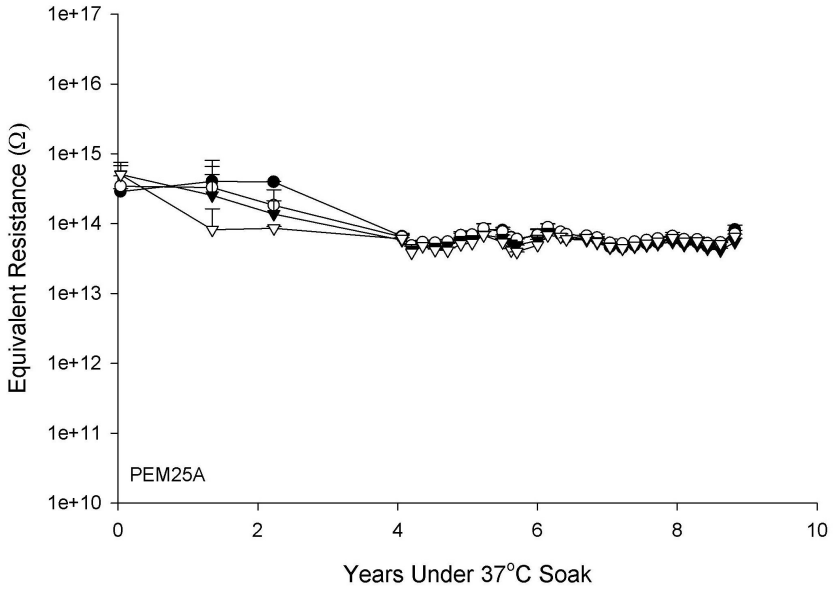

Fig. 26. Hüls PEM25 two component platinum catalyzed silica filled liquid silicone rubber. The four concentric silicon IDEs on this device are remarkably well behaved and all are still under test after 9 years of continuous 37^{O}C saline soak.

Figure 28 summarizes testing of CV2500 coated triple track devices. CV2500 is a Nusil product similar to MDX-4-4210 that is ultra-purified before delivery. All four devices have been performing well at 90°C for over 2 years, but there is no apparent difference between this material and the other MDX-4-4210 analogs for this application. Nusil MED4-4220, another analog of MDX-4-4210, performed well for 1-2 years at 90^{O}C in saline (Fig. 29). Again, if consistent with first order reaction kinetics and an activation energy of 1eV would indicate a lifetime of over 200 years at 37^{O}C.

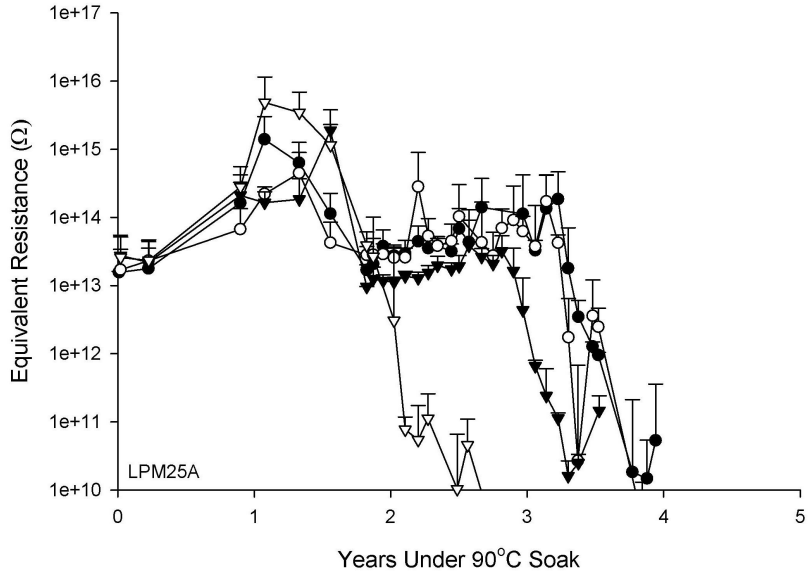

Fig. 27. 90°C saline soak test of Hüls PEM25 two component platinum catalyzed silica filled liquid silicone rubber on long silicon IDEs. Relatively consistent results for a 90°C saline soak test. Average failure time of about 3 years.

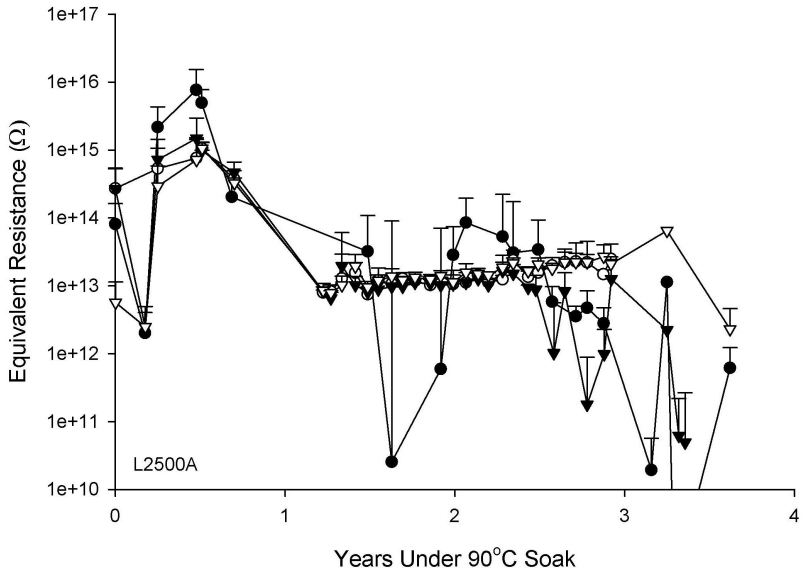

Fig. 28. 90°C saline soak test of Nusil CV2500 on silicon IDEs.

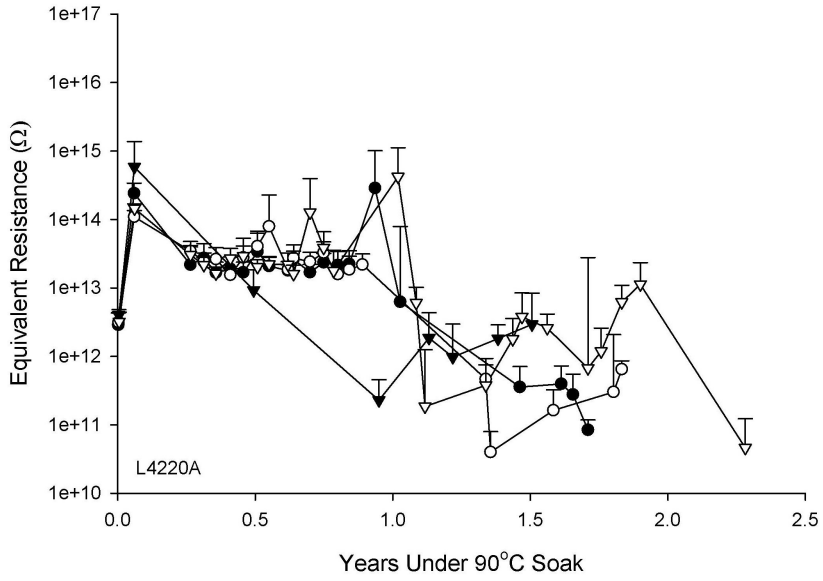

Fig. 29. Nusil MED4-4220 on silicon IDEs soaked at 90°C.

Other silicones are also under test but the general finding thus far is that all of the encapsulants similar to Dow Corning MDX-4-4210 appear to perform well as encapsulation for the silicon dioxide surfaces. However, considerable variability has been observed. Whether this is due to some subtle chemistry issues or more likely cleaning and surface preparation issues is currently under investigation.

4.1.3. In-vivo elasticity measurements for silicones

From the observation of IDE encapsulation failures for resin filled silicones such as MED6210, and observed softening of occasional materials that have failed, mechanical properties of the materials became of interest. In order to detect possible hydrolytic weakening of the silicones as was observed for Kapton/polyimides and polyurethanes by others, a simple elasticity measurement was conducted on a subset of the silicone materials under consideration. Samples were cast into 2 mm diameter rods, cured according to the standard schedule, and then implanted in animals for varying times. The results of a 4 month sequence are shown in Fig. 30. Note that all were relatively stable with the exception of MED6210. This material also rapidly failed encapsulation tests for IDEs *in-vitro*.

C Series 118 Days	Factor II 2186	Nusil CF2-3521	Nusil MED-4211	Huls PEM25	Nusil MED-6210
Pre-Implant	7,898	7,109	11,368	4,809	28,652
Post Implant	9,224	7,112	11,171	4,494	13,019
Ratio Post/Pre	1.17	1.00	0.98	0.93	0.45
Young's Modulus gm/cm^2					↑

Fig. 30. Results of one in-vivo test of elasticity using 2mm diameter rods of the various silicones listed. Note the general stability for silicones with the exception of the resin filled MED-6210.

The failure of MED6210 may be due to hydrolysis of weak resin-elastomer bonds. Precisely why this might be related to failure of the surface encapsulation test for IDEs is not fully understood but may be due to evolution of micro-voids around the filler particles which somehow coalesce on the surface of the silicon.

While not as striking as the degradation process that occurs in MED6210, other materials may also be undergoing slower mechanical changes. One widely accepted theory of silicone degradation[50] is that it is caused by a pair of competing reactions. One process is the formation of additional cross linkages which results in stiffening and hardening of the material. Tensile strength is increased generally. The second process is the de-polymerization of the material which results in softening the material. Which process dominates depends to a large extent on the conditions of aging. In the presence of oxygen and the absence of water, and particularly at elevated temperatures, additional cross linkages are formed by oxidation of the organic constituents resulting in hardening. In the absence of oxygen and the presence of water, hydrolysis of cross-linkages and chain scission may occur resulting in softening. The stability of the material at the beginning of the aging process may also impact the outcome of these competing reactions. Hydrolysis of cross linkages is a reversible process. If the molecules are hindered from physically moving apart, then the cross linkages can readily repair. Thus, a material that is initially more cross linked may in fact be more stable, or a material that becomes more cross-linked in the presence of oxygen may become more stable with time. In addition to the amount of cross linkages designed into the material, the number of cross links is also a strong function of the cure schedule over some temperature range.

To begin understanding these issues for the materials under consideration, a small matrix of pull tests of samples of a representative silicone (CF20-2186 from Nusil) were implemented. Sixteen 20cm long rods of CF20-2186 silicone were cast using 2mm diameter Teflon® tubing as a mold. Curing time was 3 hours for all cycles. All rods were cured at 50°C. Four of these rods received an additional air cure of 100°C. Four others received an air cure of 150°C. The remaining four received and additional cure of 200°C. All were then tied into loops using "fisherman's knots" to secure the ends. The resulting o-ring structures were then pull tested on a simple pull system that used a sensitive computer interfaced Mettler® balance for measurements. Measurements consisted of alternately stretching and relaxing the rings using 1/4" diameter stainless steel rods that were moved by a micro-stepping linear actuator. The resulting slope of the force-displacement curves were then used to compute Young's modulus (Fig. 31).

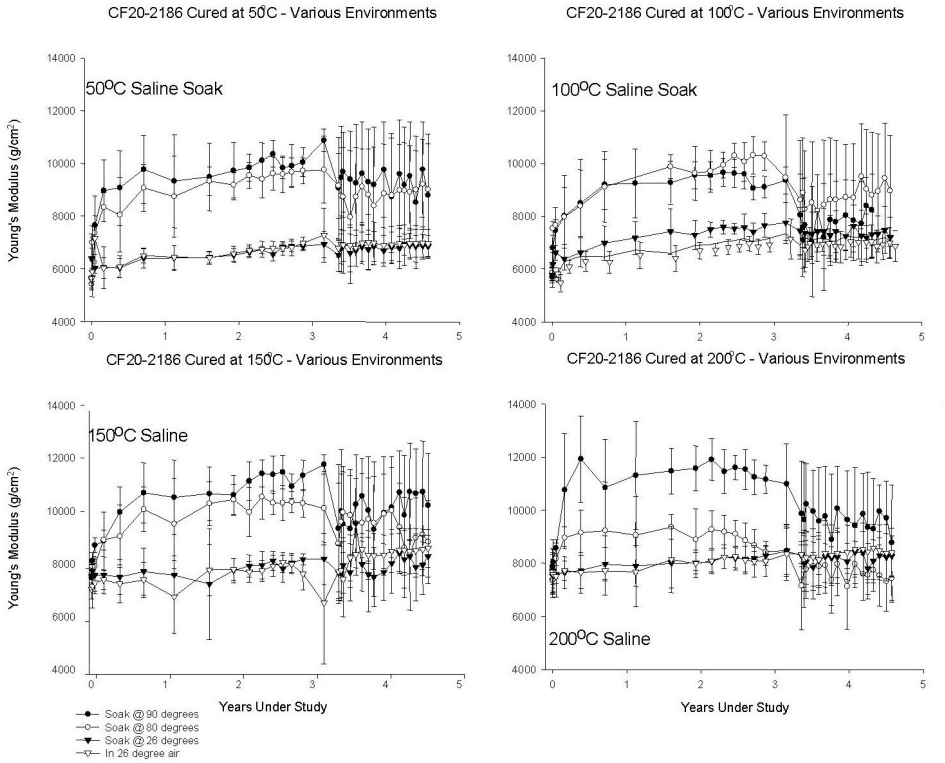

Fig. 31. Young's modulus versus aging in days under various conditions for samples of Nusil CF20-2186 cured under various conditions.

One loop from each cure schedule group was placed in one of four environmental conditions: 1) 90°C saline, 2) 80°C saline, 3) 26°C saline, and 4) 26°C air. Periodically the loops were withdrawn from the aging environments and pull cycled. As shown in Fig. 31, there is considerable variability in the data, but in general, there appears to be a stiffening of the material with time that is accelerated by elevated temperature saline soaks. After several years, there appears to be a convergence of elasticity in some sets. One device failed after turning a milky white color.

The relationship between the cure schedule and elasticity is shown in Fig. 32. Apparently there is a non-linear effect of cure temperature on the elasticity of the silicones which may be significant for applications. These experiments are just beginning, but the method appears to be useful and may define proper cure schedules for silicones used as insulating biomaterials. Once the *in-vitro* work is well along, a series of animal experiments will also be undertaken to determine if similar effects occur in the complex biochemistry of the body.

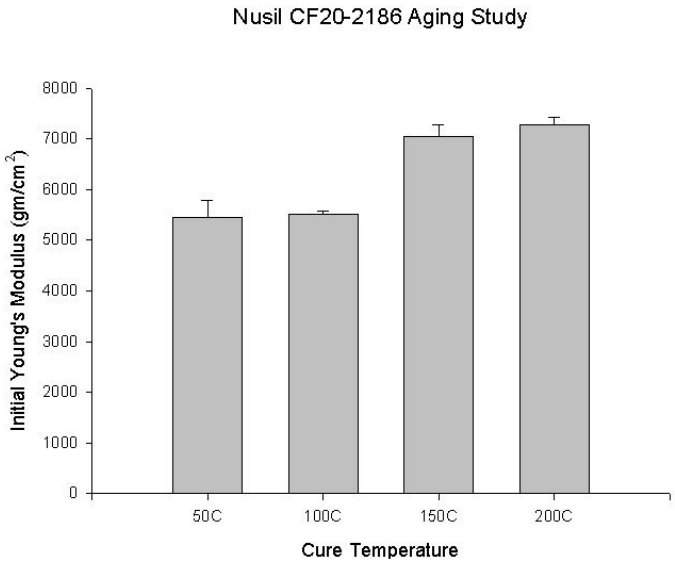

Fig. 32. Initial elasticity modulus prior to aging for Nusil CF20-2186 samples cured at different temperatures. There were 4 samples in each group. Error bars are 1 standard deviation.

4.1.4. Silicone adhesion testing

New methods are being developed for documenting cleaning procedures suitable for long term encapsulation work. Previously, for consistency, an aggressive approach to cleaning has been used prior to coating. It is difficult to know, however, what the minimum clean is to get good results. This would be valuable knowledge for other labs since cleaning procedures are costly, and aggressive cleaning procedures greatly limit the type of substrates that can be used. More importantly, perhaps, a set of standards for cleaning and verifying surface preparation can be developed. Direct adhesion testing may be one means of accomplishing this goal. However, there are subtleties to adhesion testing. In an initial test, peel forces were measured but the rate of pull did not appear to let the material settle as shown in Fig. 33**A**. By slowing the rate of stretching from 100 µ/sec to 10 µ/sec, the record was substantially improved as shown in Fig. 33**B**. The resulting data was remarkably consistent following an initial transient that was likely due to release of the tape used to attach to the silicone (it was double sided tape and the backside was attached to the substrate with the silicone attached to the front side).

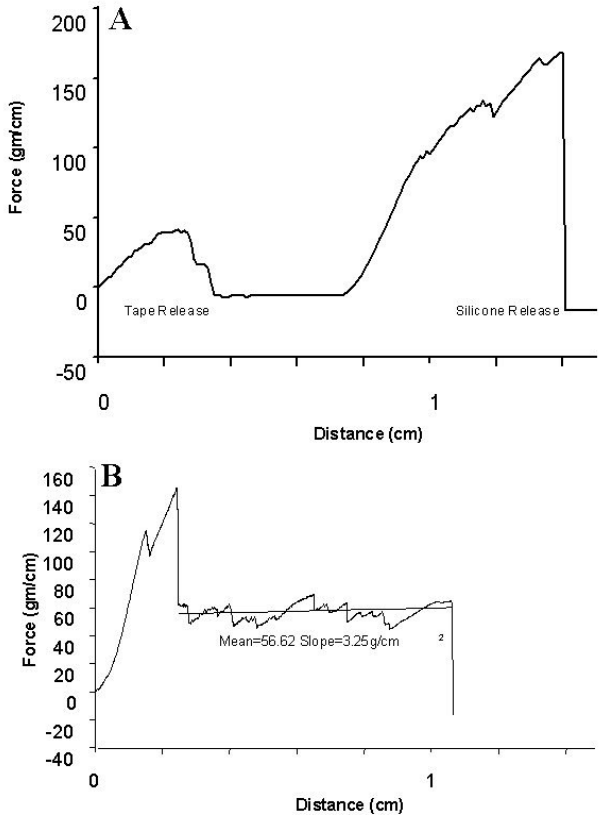

Fig. 33. Silicone peel test examples on uncleaned silicon chips using fully cured Nusil CF20-2186. Note long, near zero slope exhibited by data in B**, taken from a pull test with a very slow pull rate compared to the data shown in** A**.**

A variety of samples were prepared with different surface cleaning protocols, and cure schedules to identify critical points in silicone encapsulation methodology. This information will allow preparation of more consistent samples, and will improve the odds that other laboratories will be able to duplicate the results using silicone encapsulants. Five samples were prepared using portions of silicon chip cleaning protocols used to generate most of the data in the insulating biomaterials program, followed by application of a 0.5 cm wide stripe of Nusil MED-4220. The stripe of silicone overlapped a piece of Kapton tape with double sided silicone adhesive.

The simplest clean consisted of "Pirhana" etch (2:1 conc H_2SO_4:30% H_20_2) followed by a de-ionized water rinse and N_2 blow dry. Results of this test are shown in Fig. 34. The adhesion force exceeded the tensile strength of the material (431 gm/cm) in contrast to the 56 gm/cm adhesion strength measured for samples that were not cleaned prior to application of the silicone. Other samples that were tested had additional steps added to the basic clean: Pirhana plus isopropyl alcohol and N_2; Pirhana, isopropyl alcohol, N_2, and 150°C bake; Pirhana, isopropyl alcohol, N_2, 150°C bake and 30 min UV-Ozone; and finally the complete clean of Pirhana, isopropyl alcohol, N_2, 150°C bake and 10 min UV-Ozone. All of the samples exceeded the tensile strength of the silicone.

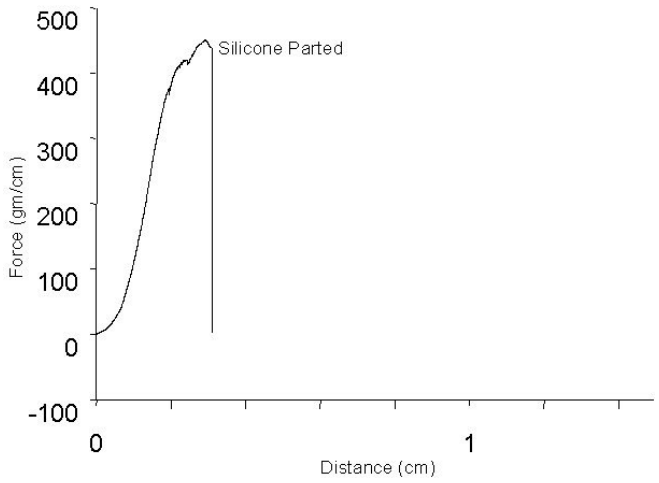

Fig. 34. Pull test of sample prepared with only Pirhana clean and DI rinse. Adhesion exceeded the tensile strength of 0.5 cm wide by ~1 mm thick silicone piece.

Thus the good news of these experiments is that an aggressive surface cleaning is sufficient to substantially improve the bonding of silicone to the silicon dioxide surfaces. However, the methodology was insufficient to allow further differentiation of the effects of surface preparation. Additional experiments using fiberglass reinforced peel strips are in progress.

4.2. Use of fluorocarbons as an implantable material

Compared to silicones, relatively little has been published on the use of Teflon® as an implantable material. Cell culture studies indicate that it is compatible with neurons and other CNS elements[1].

Teflon® aortic implants received poor reviews by a number of clinicians in the 1970's. However, retrospective study[10] showed that the fault was with the use of silk sutures and choice of weave, not with the Teflon® itself. In one example, PolyTetraFluoroEthylene (PTFE) aortic grafts implanted as long as 19 years previously revealed that grafts had increased dimensions by about 10% and lost about 10% in mechanical strength. The PTFE fibers showed no other evidence of changes under SEM examination. The same paper also describes animal implants which also revealed no degradation of the Teflon® grafts. In contrast, Dacron® grafts showed considerable degradation over time. This indicates that Teflon® may remain functional as a material over long times *in-vivo*.

When Teflon® is used as a load bearing component of an implant, such as a joint surface in an artificial hip, disastrous effects occur. As Teflon® particulates are released into the tissue, a large scale inflammatory response resulting in formation of a granuloma can be triggered[61].

4.2.1. In-vitro evaluation of Teflon® insulation

Previous work on evaluation of Teflon® PerFluoroAlkoxy (PFA) insulations showed that for properly coated wires, no loss of resistive properties were observed for over 5 years of biased soak in saline. However, the system being used at that time was only capable of detecting leakage currents down to 1 pA with wire lengths of only 8 cm. Also, the instrumentation used in that system was sensitive to ambient humidity changes which further reduced the overall accuracy of the measurements.

New samples of PFA coated wire were used to create 1 cm diameter spools of wire for testing. In order to improve the sensitivity of detection, 60 cm long pieces of wire were under soak to provide a total surface area of approximately 2 cm^2. The 1 cm spools were designed to place mild compression and tension stresses on the wire insulation to expose any mechanical issues such as were found for

Kapton/polyimide and polyurethane coatings. Samples were mounted in the bottom of long tubes under saline held at 90°C. Initially, the single measurement system was used until the continuous measurement system was available near the end of year 2. An example of typical results from PFA insulation testing are shown in Fig. 35.

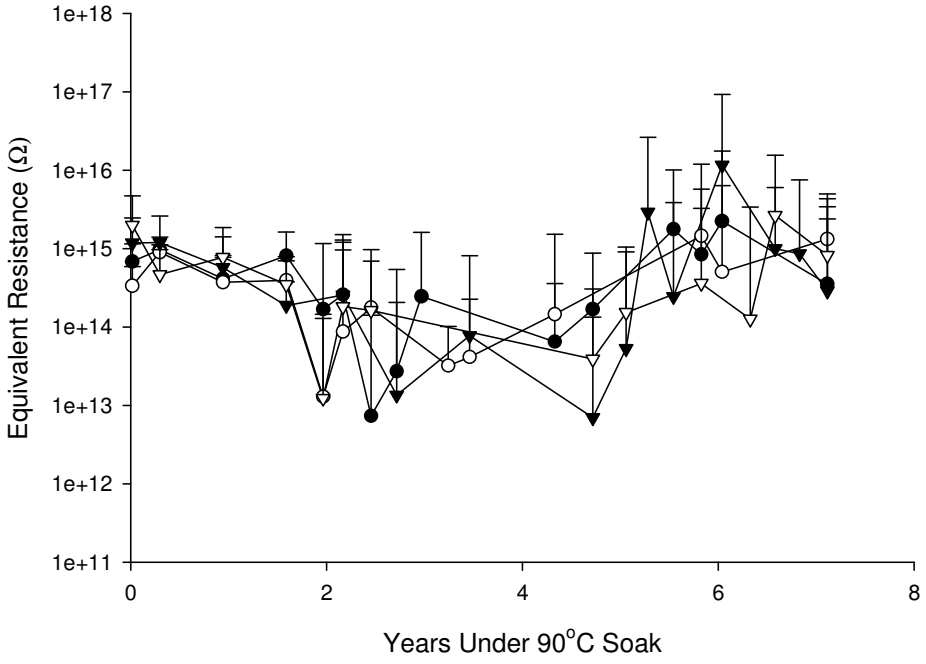

Fig. 35. Sample SP3GTA 60cm long, 75µm diameter gold wire with 18µm PFA coating. Data was non-uniformly sampled during one year averaging time periods. Error bars are shown as positive only due to log scale and are 1 standard deviation as computed from actual variance of data within each period. Numerous system changes may have been responsible for variable data from years 2-5.

Assuming a bulk resistivity of $1x10^{18}$ Ω (at room temperature), a resistance reading of about $1x10^{15}$ Ω would be expected for these samples. The observed reading of $1x10^{14\text{-}16}$ Ω is close considering that these measurements are taken at 90°C which enhances many processes of electron transport over room temperature measurements.

PFA insulation has only failed when there was inclusion of a defect in the sample being tested or an error in assembly. PFA is an outstanding insulating biomaterial. There are some cautions, however. Some manufacturers use dispersion coatings to produce insulating films. If not properly re-flowed, then pinholes or even porous films can result. Also, one of the reasons why PFA performs so well as a wire insulator is that it is concentric about a uniform cylinder. PFA, by its chemical nature has no capacity to form covalent bonds with any of the surfaces of interest. However, as an insulator of wire, it is by many orders of magnitude the best that has been tested.

4.3. In-vivo evaluations

Over 40 animals were implanted with a variety of test devices placed subcutaneously or subdurally. Biasing battery capsules were mounted on the percutaneous connectors and worked well. Unfortunately, most of the soft tissue percutaneous connectors marsupialized within about 8 months or less and were destroyed when the animals chewed the implanted devices. However, several devices were implanted under the paraspinal fascia in an effort to block the epithelial downgrowth with the fibrous tendon. This

was attempted after it learned from dental literature that fibrous materials were being used successfully to block epithelialization of the roots of teeth following periodontal repairs. These particular devices were successful and have been monitored for up to 3.5 years. Most of the subdural implants were lost due to the animals apparently banging the connectors on the caging when startled. Current results are summarized in Table 1.

Subcutaneous IDEs implanted over the hip consisted of four interdigitated electrode arrays (IDE arrays) mounted on titanium percutaneous connectors. Only two survived for several years. These devices had continuous 6 V battery voltage applied between the traces of the IDE arrays. Wire loop implants consisted of 1 cm long loops of wire implanted subdurally and leading through the skull to a percutaneous connector. Sub-dural IDE devices consisted of two IDE arrays implanted subdurally with lead wires through the skull to a percutaneous plug. Channels 8 and 10 were not functional in these implants since there were only 2 IDE arrays/connector.

Silicone encapsulated IDEs survived for over 4 years before the last connector failed. The silicones used correspond to the animal ID. Implant R4211B was coated with Nusil MED-4211. Implant R2186B was coated with Nusil CF20-2186. Implants R4220B, C were coated with Nusil MED-4220. Implant R2500C was coated with Nusil CV2500, a low volatiles/ultrapure silicone. The R4211B and R2186B implants together have only exhibited one failure of 8 devices ($<10^9$ Ω) over the nearly 4 year test period, and this failure occurred at the beginning of testing. The IDE readings indicate a surface resistivity of between 1E16 to 1E18 Ω/sq. The newer subdural IDE implants exhibited similar performance. The PFA coated wire loops also exhibited excellent results with one device still under test after 5.4 years with an intact connector.

While this table has become far smaller than originally planned, useful animal data was obtained. The totally implantable, high sensitivity, multichannel electrometers that transmit data across the skin with no percutaneous connectors will solve all of the issues that have thus far limited this portion of the insulating biomaterials research. These devices will be very similar to the PassChip described above, and will perhaps revolutionize the ability to gather this critical data.

Table 1. Summary of subcutaneous IDE implants over the hip (SQIDE) sub-dural wire loop implants (SDWIRE), and sub-dural IDE implants (SDIDE) in rabbits.

ID	DEVICE	INSULATION	YEARS	OHMS-4	OHMS-6	OHMS-8	0HMS-10	FAILURE
R3PITA	SDWIRE	PFA	5.4	5.46E+12	3.86E+12	2.64E+12	4.47E+12	None
R4220C	SDIDE	PtSilicaSilicone	4.1	>2e14	3.41E+13			Connector
R4211B	SQIDE	PtSilicaSilicone	3.9	1.41E+13	7.45E+11	4.69E+10	5.07E+11	Connector
R2186B	SQIDE	PtSilicaSilicone	3.7	<1e9	2.73E+13	2.35E+13	1.97E+14	Connector
R2PT3A	SDWIRE	PFA	1.7	1.97E+14	1.02E+14	7.04E+13	<1e9	Connector
R4220B	SDIDE	PtSilicaSilicone	1.2	>2e14	<1e9			Connector
R2500C	SDIDE	PtSilicaSilicone	1.0	1.79E+13	<1e9			Connector
	SDWIRE = Subdural Wire Loops							
	SDIDE = Subdural IDEs							
	SQIDE = Subcutaneous IDEs							

4.4. Other materials and tests

4.4.1. Thin film ceramics

Thin film ceramics are needed to provide ion and water barriers to protect CMOS integrated circuits under soak conditions. Typically, semiconductor manufacturers rely on silicon nitride for that function. Ongoing tests have shown that silicon nitride is susceptible to dissolution when subjected to biased soak conditions. This behavior of silicon nitride was documented in the late 1960s during experiments for developing ways to etch silicon nitride for the electronics industry[55,59]. Many attempts at defining the limits of this process, and to identify possible alternatives have been undertaken. A set of test devices that take advantage of the silicon wafer bulk resistance test configuration have yielded reliable data. These test structures consist of small silicon wafers that have been coated with the materials listed below. Wires are attached to the wafer

backs and the entire assembly is potted in silicone except for a round window, 6 mm in diameter, over the film under test. Four of these are then assembled into long tubes and placed under heated soak conditions at 90°C to accelerate what appears to be a chemical process.

- 1,000Å LPCVD silicon nitride on bare silicon.
- 5,000Å PECVD silicon nitride on bare silicon.
- 1,000Å LPCVD silicon nitride over 1,000Å thermal oxide.
- 5,000Å PECVD silicon nitride over 1,000Å thermal oxide.
- 5,000Å LTO deposited oxide over 1,000Å LPCVD silicon nitride on bare silicon.
- 5,000Å LTO deposited oxide over 5,000Å PECVD silicon nitride on bare silicon.
- Bare silicon coated with Nusil CV2500 for a control.

All of the 1,000Å LPCVD silicon nitride coatings on bare silicon failed in less than 7 months under ±5 volt continuous IV sweep measurements. Two of the 5,000Å PECVD silicon nitride on bare silicon samples failed in approximately 9 months with two surviving up to 18 months. Similar behavior was observed for the remainder of the devices with the exception of the two types that have 5,000Å LTO (Low Temperature Oxide) overcoating the silicon nitride layers. The LTO layer apparently stabilizes the silicon nitride films sufficiently to extend the protective properties to over 5 years in some cases. This appears to verify the hypothesis that silicon dioxide somehow may stabilize the silicon nitride layer if it is applied to the outer surface. Notably, very thin films of silicone applied to silicon nitride also appear to protect the silicon nitride. Thus it may be that LTO or a plasma deposited silicone can be used to stabilize silicon nitride which can then be used as a reliable, long term ionic barrier for CMOS circuits.

4.4.2. Silicon corrosion tests

A variety of surface tests were performed including implantation of double polished silicon pieces coated on one side by silicone. The original intent of this was to allow infiltration of biochemicals which could then be detected by differential FTIR spectroscopy. However, removal of the silicon pieces after 6 months revealed that the unprotected backside of the silicon had corroded to such an extent that the FTIR measurements could not be completed, while the silicone coated front side was unaltered. This may indicate that silicon must be protected in some way to avoid corrosion. Since the University of Michigan program's devices had no protection for the underlying silicon substrate, this finding was significant. However, corrosion of UM devices had not been reported, so to determine if the P^+ substrates were somehow inherently corrosion proof, some example devices were obtained for testing. Devices were implanted subcutaneously and in the subdural space of a New Zealand rabbit and left in place for nearly one year. None of the devices showed any evidence of corrosion of the substrate. In fact, the micro-etch pattern left by the boron etch stop process used to fabricate these probes remained as well. There was some evidence of corrosion of the front surface of the structure evidenced by a rainbow effect on the dielectrics that was not previously noted. Additional studies indicate that lightly doped silicon dissolves at a rate of approximately 1 µm/month indicating the need for some form of corrosion protection for the backside of implantable integrated circuit devices.

4.4.3. Solder joint tests

Simple solder joints were a significant factor in the reliability of long term test devices. Part of the problem was caused by the need to join a variety of metals — gold, silver, platinum, platinum-iridium — to brass connector pins, or copper extension wires. While all joining methods were tested, they were not long term tested and were not always tested at all temperatures such as those encountered in the autoclave. After considerable effort to identify a reliable solder for gold, indium solder was chosen which had sufficiently

high melting point to be safe for autoclave temperatures. Occasional faults in devices fabricated with indium solder were found and these appeared more frequently with time and after autoclave. In order to avoid additional failures from solder joints, all of the joining methods in use were placed under test in order to determine a minimum set of methods that could be counted on for long term testing.

Twenty-two long tube assemblies were constructed to test the reliability of various joining methods with various wire types. The basic idea of the solder test is shown in Fig. 36. Wires were held in silicone tubes to ensure a 0.012 in. or greater gap to test the solder and the solder-wire interface without the possibility of wires touching directly. This entire structure was then encapsulated in CF20-2186 silicone and immersed in 90^0C saline for testing. Wires were Teflon® coated. To join the wires to the connector, they were first brazed to silver wire which was then soldered with standard lead-tin solder to Teflon® insulated multistrand hookup wire. This solder joint was placed high in the tubes to minimize heat. Also, the brazed/soldered joint was placed under soak test at 90^0C to test the reliability of that method as well. A matrix of all possibilities of silver, gold, platinum, platinum-iridium, hook-up wire and indium solder, lead-tin solder, lead-tin-silver solder, silver epoxy, silver silicone were created and placed under test.

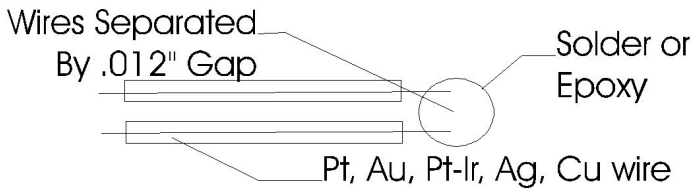

Fig. 36. Solder tester. Wires are joined by solder alone, wires do not touch within blob of solder.

As shown in Table 2, platinum-iridium is more difficult to reliably join than other metals using most techniques. Silver wire is also very difficult to join reliably. Silver silicone is very unreliable, indium solder is unreliable, but the rest are promising depending on the wire being joined. It may be that to join gold reliably a brazing method will need to be used. While mundane information, this chart may help avoid needless failures for long term soak assemblies and implantable devices.

Table 2. Solder - Wire 90ºC saline soak summary showing fraction that have not doubled solder joint resistance readings after 2.5 years.

Solder \ Wire	Gold	Silver	AgCu Multi-strand	Platinum	Pt-Ir
Indium Solder	4/6	0/6	3/6	0/6	0/6
H20E Ag Epoxy	2/6	5/6	6/6	1/6	0/6
Sn63Pb37 Solder	na	0/6	6/6	¾	6/6
Sn62Pb36Ag2 Solder	na	3/6	6/6	5/5	2/6
Sn98Ag2 Solder	na	na	na	4/4	na
Silver Silicone	0/6	6/6	na	0/5	0/6

4.4.4. Short term polymer flexible interconnects

One of the pressing needs for an insulating biomaterial is a substrate for micro-ribbon interconnects that can be used to interconnect University of Michigan silicon microelectrode arrays with percutaneous

connectors. Silicon cables are fragile and at present may be unable to withstand the forces generated by healing tissues such as dura, skull, and periosteum. A more robust cable is needed to interconnect a skull mounted percutaneous connector and a sub-durally implanted silicon microelectrode array with integral micro-ribbon.

Polyimide based micro-ribbon cables are being developed for providing interconnection between the silicon micro-ribbon/microelectrode array and the skull mounted percutaneous connector. Polyimide is known to be a poor insulating biomaterial for long-term implants because of relatively rapid degradation in aqueous environments. However, polyimide is one of the few flexible substrate materials for which there is an established micro-fabrication technology. Mylar® (polyester) is another choice, but Mylar® also exhibits similar long term deficiency.

For short-term implants, perhaps up to one year, polyimide may be sufficiently long lived to provide an interim solution. Kapton based interdigitated test structures insulated with various materials have been evaluated. Only devices that were completely encapsulated in one of several epoxies showed promise. All acrylic and epoxy sandwich structures failed rapidly in water soak tests due to diffusion of water into residual spaces left during the assembly process. Also, all silicone insulated structures failed rapidly.

The University of Michigan National Center for Neural Communication Technology (Jamie Hetke) has fabricated several test devices with a commercially produced mini-ribbon cable that use standard Kapton sandwich structures with acrylic adhesives. Several of these assemblies were tested, and all failed rapidly by similar mechanisms. An additional note is that the copper traces on all commercially fabricated test ribbons darkened during soak testing indicating that oxidation of the copper traces was taking place in spite of the acrylic/Kapton sandwich structure.

Gary Roughton in Dr. Nagle's lab at North Carolina State University prepared five different Kapton based interdigitated electrode arrays to test various approaches to preparation of implantable Kapton based structures. All structures were formed by deposition of gold traces on Kapton substrates followed by coating with an insulator. The insulators used were Dow Corning silicone T-RTV, Dupont Polyimide 2721, Dupont Polyimide 2723, Dupont PC1025, and Dupont Dow3-1753. Initially, samples were dry tested for 3 weeks before the addition of saline to establish a baseline of bulk resistivity. Following addition of saline, many samples survived for an additional 2 weeks. The Dupont Polyimide 2721 coated samples were the most reliable. And have survived for over 6 months thus far.

The graphs shown in Fig. 37 were constructed using measured data from the surviving structures and results of the simple model shown in Fig. 38. The test structures were interdigitated electrode arrays on Kapton substrates with Dupont 2721 Polyimide overcoating the electrodes. They were provided by Troy Nagle's lab at North Carolina State University (NCSU). The four test structures were well matched and were implemented when the continuous test system was relatively stable.

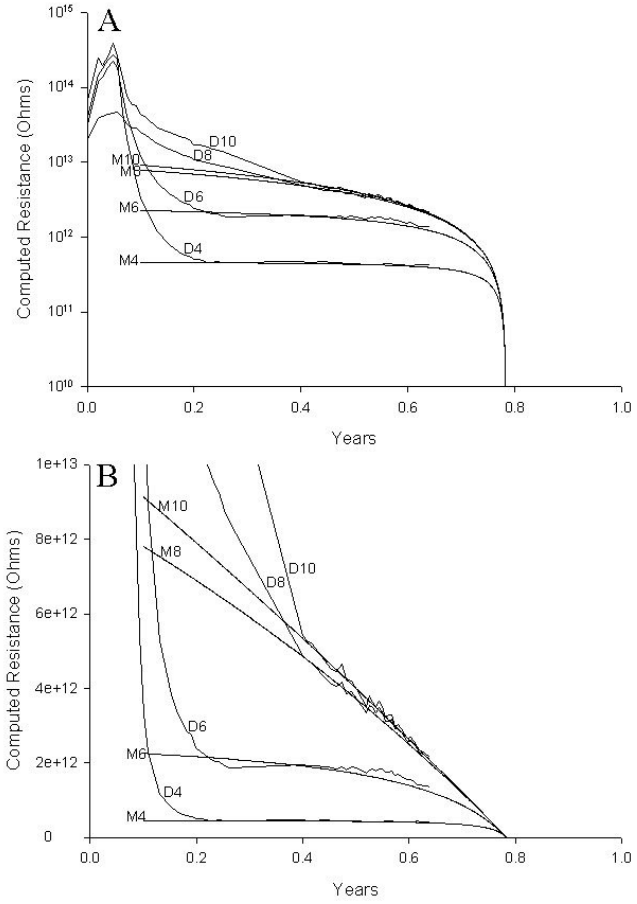

Fig. 37. Data (D) from Kapton/Polyimide mini-ribbon cable process from NCSU interdigitated electrode arrays shown on log and linear scales together with data from simple parallel resistance model (M).

The model, as shown in Fig. 38, consisted of a constant resistance (R_C) in parallel with a second resistance that was time dependent. This time dependent resistance was modeled using an equation found by performing a linear regression on the most recent three months of data. The recent data was used because the effects of the initial transients caused by hydration had settled out for the most part. Also, it was where the contribution from the parallel constant resistances would be as low as possible.

For the lower resistivity devices, the constant resistance term was estimated from the middle segment of the data which was fairly constant over time for the devices that exhibited the highest leakage initially. Because there was no clear region where the resistance didn't change for Electrometer 8 and 10 devices, the constant resistance term in the model was adjusted to provide an adequate fit to the data at the 0.5 year mark where the last linear data segment joined the middle, flat segments.

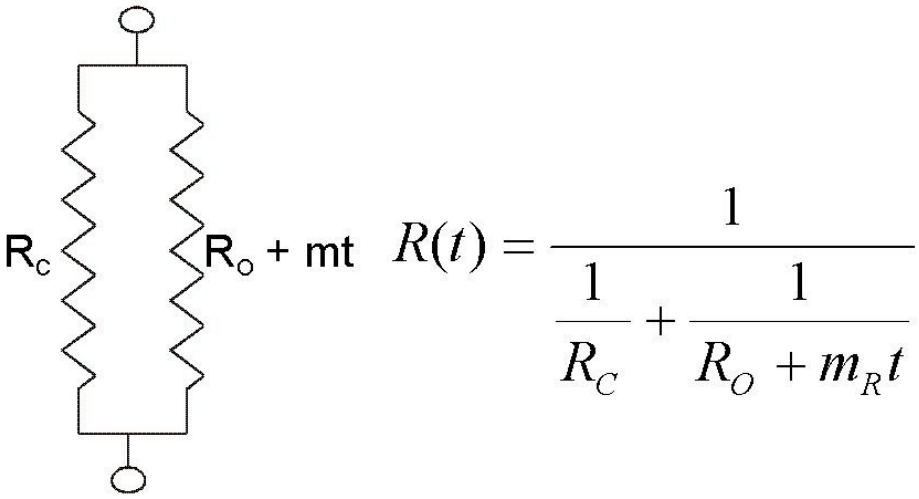

Fig. 38. Simple model for observed data from Kapton soaks consisting of a constant resistance in parallel with time dependent resistor.

The resulting model data fit the last segment of the real data well as it should. It may be that if there truly is a degradation process that begins as a high resistance and falls over time as evidenced by the high resistance devices, there will be an apparently sudden demise of the low resistance devices at about 0.77 years. The apparent rapid demise of the devices after about 0.7 years is actually due to the increasing dominance of the time dependent resistance term as the it becomes equal to and then lower than the constant term. In fact, from prior work on wire samples coated with polyimide, there is a relatively sudden failure mode at about 8 months following saline immersion.

This example illustrates a subtle problem with lifetime testing and estimation. There is no way to determine if one parameter is masking a second process until the second process progresses far enough to be observable. That is, if all of the devices had the same low value constant resistance that Electrometer 4 exhibited, there would have been no way to tell that the second process was occurring. Thus, until the second process becomes visible, any predictions based on the data would grossly overestimate the lifetime of the device. Constant awareness of the potential for masking of degradation processes can help minimize the risk of having implantable devices fail "out of the blue" because an unrecognized process had not been elicited during testing.

4.5. Commercial materials – summary of results

A wide variety of materials have been evaluated for lead insulation *in-vitro* with only silicones, fluorocarbons, and one polyesterimide exhibiting sufficient longevity for further investigation *in-vitro* and *in-vivo*. Bending tests and bonding tests have shown that fine platinum wire may be the ideal interconnect material since it is more flexible than gold wire of the same tensile strength. However, insulated wire of very fine diameters is not currently available commercially. Plasma deposited insulators may be one solution for insulating the fine wire interconnects which is discussed in detail in Chapter 3.3.

Many materials have been evaluated for encapsulation of silicon surfaces for protection of lead bond areas and exposed traces. Only some silicones have exhibited any capacity whatsoever to accomplish this task. Fortunately, these silicones have successfully insulated test structures for over 12 years of continuous biased saline soak. Temperature acceleration and *in-vivo* testing for over 6 years have further verified the functionality of these silicones. Pull tests of 1 mm diameter silicone samples have revealed that while most silicones maintain stable elasticity during long-term saline immersion and long-term subcutaneous implantation, some rapidly degrade. It appears that the difference may be related to the filler

used. The samples that degraded were fabricated with optically clear silicones that utilize resin filler for optical clarity. The samples that maintained their elasticity were fabricated with fumed silica filler. The elasticity property is sensitive to cure conditions that may indicate that chemical-structural changes can occur under some cure conditions that may not be observed with other cure conditions. Further investigation of these observations is needed to avoid the pitfalls found during polyimide and polyurethane testing discussed above.

Teflon® (mostly PFA but others as well) has exhibited the highest insulation resistance for the longest time of all materials tested. Other than failures related to defects in the films, Teflon® insulated wire exhibits no signs of degradation over many years of *in-vitro* saline soaks at all temperatures. Similar success has been found during animal tests for over 5 years thus far. Unfortunately, Teflon® does not adhere to silicon dioxide surfaces, and thus cannot be used to protect the bond area of an implant. However, Teflon® wire can be overcoated with silicone elastomers to form a permanent "o-ring" like seal that seems to perform well indefinitely. Thus a 2 part system with Teflon® insulated wiring and silicone encapsulated bond areas is recommended at the present time for long term animal implant assembly. Dozens of structures have been fabricated using this approach and have verified the performance *in-vitro* in 37^{O}C and 90^{O}C saline, and *in-vivo* for over 5 years. However, use of larger gauge (30 awg or larger) pigmented Teflon® insulated wire with silicone insulation has not been effective at elevated temperatures or *in-vivo*. Apparently, a small virtual space forms between the Teflon® on the wire and the silicone encapsulant which can lead to failures if the insulated wires touch within the silicone overcoat. Also, there are legal prohibitions for clinical applications due to prior litigations involving use of Teflon® as a structural implant element.

Ceramic coatings such as silicon dioxide and silicon nitride are of particular interest and were extensively tested. Thin films of thermal silicon dioxide become conductive when immersed in saline solutions. Silicon nitride dissolves slowly when immersed under bias in saline solutions. However, it was also discovered that inclusion of a thermal oxide layer under the silicon nitride layer slowed the dissolution. Application of a very thin film of silicone or silicon dioxide over the surface of the silicon nitride layer further reduces the dissolution process. This was an important discovery because silicon nitride is an excellent sodium barrier for CMOS integrated circuits.

5. Conclusions

A variety of issues have been discussed. On a cautionary note, the results presented here are quite preliminary in spite of the relatively long term testing that has so far been accomplished. As evidenced by the results observed for the PassChip implants, in spite of current knowledge, assembled systems fail quite readily for a variety of reasons. Substrates must be clean to achieve repeatable results otherwise there may be a three part structure – the substrate, the encapsulant, and the contaminating material in between. Also, what works on one substrate may not work on another substrate because of the different interfacial chemistries involved.

Silicones are an excellent class of materials to consider for protection of silicon dioxide or metal oxide coated systems. Silicones appear to provide outstanding corrosion protection of silicon and other oxidizable materials perhaps because the bonds formed are quite strong and thus stabilize the surface molecules. Fluoropolymers, while quite excellent insulators and quite stable in biological systems, have limited application due to the inherent need for a transition between a fluoropolymer and a silicone encapsulation as fluoropolymers do readily not adhere to other surfaces, particularly under hydrated conditions. However, there is ongoing work to improve the attachment of fluoropolymers to other materials which may someday provide a solution to this issue. CMOS integrated circuits seem to function well with minimal protective coatings as long as the protective coatings are stabilized by silicone encapsulation. Polyimides thus far tested are suitable for relatively short term applications or for applications where some cracking and increased conductivity can be tolerated. Parylene is similar though some new forms of Parylene may perform better than Parylene N or C.

Acknowledgements

The long term support of this work by Drs. Terry Hambrecht and Bill Heetderks with the NIH Neuroprosthesis program is sincerely appreciated.

References

[1] Ammar, A., C. Lagenaur, and P. Jannetta. Neural tissue compatibility of teflon as an implant material for microvascular decompression. *Neurosurg. Rev.* 13:299-303, 1990.

[2] Aylett, B. J., R. E. Clegg, and P. E. Donaldson. Hydrothermally stable bonding of silicone rubber to titanium. *Med Biol Eng Comput* 34:394-5, 1996.

[3] Bakker, D., C. A. vanBlitterwijk, S. C. Hesseling, W. T. Daems, and J. J. Grote. Tissue/biomaterial interface characteristics of four elastomers, a transmission electron microscopical study. *Journal of Biomedical Materials Research* 24:277-293, 1990.

[4] Bogoch, E. R. Silicone synovitis. *Journal of Rheumatology* 14:1086-1088, 1987.

[5] Brindley, G. S., and P. E. Donaldson. Electrolytic current-control elements for surgically implanted electrical devices. *Med Biol Eng Comput* 24:439-41, 1986.

[6] Brindley, G. S., P. E. Donaldson, M. A. Falconer, and D. N. Rushton. The extent of the region of occipital cortex that when stimulated gives phosphenes fixed in the visual field. *J Physiol (Lond)* 225:57P-58P, 1972.

[7] Campbell, P. K., R. A. Normann, K. W. Horch, and S. S. Stensaas. A chronic intracortical electrode array: Preliminary results. *J. Blomed. Mater. Res.: Applied Biomaterials* 23:245-259, 1989.

[8] Chardack, W. M., A. A. Gage, and W. Greatbatch. Surgery. *Surgery* 48:643-, 1960.

[9] Christ, F. R., D. A. Fencil, S. V. Gent, and P. M. Knight. Evaluation of the chemical, optical and mechanical properties of elastomeric intraocular lens materials and their significance. *J. Cataract Refract. Surg.* 15:176-184, 1989.

[10] Coutre, J., R. Guidoin, M. King, and M. Marois. Textile teflon arterial prostheses: how successful are they? *Canadian Journal of Surgery* 27:575-582, 1984.

[11] Cruz, N. I. Current ststus of silicone breast implants. *Bol. Assoc. Med. P. Rico - Agosto*:326-328, 1991.

[12] Cuddihy, E. F., J. Moacanin, and E. J. Roschke. In vivo degradation of silicone rubber poppets in prosthetic heart valves. *J. Biomed. Mater. Res.* 10:471-481, 1976.

[13] Delasi, R., and J. Russell. Aqueous Degradation of Polyimides. *J Appl Polym Sci* 15:2965-, 1971.

[14] Diamond, B., B. Hulka, N. Kerkvliet, and P. Tugwell. Silicone Breast Implants in Relation to Connective Tissue Diseases and Immunologic Dysfunction. Michigan: National Science Panel, 1998.

[15] Dolezel, B., L. Adamirova, Z. Naprstek, and P. Vondracek. In vivo degradation of polymers. I. Change of mechanical properties in polyethylene pacemaker lead insulations during long-term implantation in the human body. *Biomaterials* 10:96-100, 1989.

[16] Dolezel, B., L. Adamirova, P. Vondracek, and Z. Naprstek. In vivo degradation of polymers. II. Change of mechanical properties and cross-link density in silicone rubber pacemaker lead insulations during long-term implantation in the human body. *Biomaterials* 10:387-92, 1989.

[17] Donaldson, P. E. The encapsulation of microelectronic devices for long-term surgical implantation. *IEEE Trans Biomed Eng* 23:281-5, 1976.

[18] Donaldson, P. E. Encapsulating microelectronic implants in one-part silicone rubbers. *Med Biol Eng Comput* 27:93-4, 1989.

[19] Donaldson, P. E. Aspects of silicone rubber as an encapsulant for neurological prostheses. Part 1. Osmosis. *Med Biol Eng Comput* 29:34-9, 1991.

[20] Donaldson, P. E. Acidity of single-part alkoxy-cure silicone rubber DC3140. *Med Biol Eng Comput* 33:347-9, 1995.

[21] Donaldson, P. E. Aspects of silicone rubber as encapsulant for neurological prostheses. Part 3: Adhesion to mixed oxides. *Med Biol Eng Comput* 33:725-7, 1995.

[22] Donaldson, P. E. Aspects of silicone rubber as encapsulant for neurological prostheses. Part 4: Two-part rubbers. *Med Biol Eng Comput* 35:283-6, 1997.

[23] Donaldson, P. E., and B. J. Aylett. Aspects of silicone rubber as encapsulant for neurological prostheses. Part 2: Adhesion to binary oxides. *Med Biol Eng Comput* 33:289-92, 1995.

[24] Donaldson, P. E., and E. Sayer. Silicone-rubber adhesives as encapsulants for microelectronic implants; effect of high electric fields and of tensile stress. *Med Biol Eng Comput* 15:712-5, 1977.

[25] Donaldson, P. E., and E. Sayer. Osmotic pumping of non-hermetic neuroprosthetic implants. *Med Biol Eng Comput* 19:483-5, 1981.

[26] Donaldson, P. E., and E. Sayer. A technology for implantable hermetic packages. Part 2: An implementation. *Med Biol Eng Comput* 19:403-5, 1981.

[27] Donaldson, P. E., and E. Sayer. A technology for implantable hermetic packages. Part 2: Design and materials. *Med Biol Eng Comput* 19:398-402, 1981.

[28] Drake, K. L., K. D. Wise, J. Farraye, D. J. Anderson, and S. L. BeMent. Performance of Planar Multisite Microprobes in Recording Extracellular Single-Unit Intracortical Activity. *IEEE Trans. Biomed. Engr.* 35:719-732, 1988.

[29] Edell, D. Minisymposium: Tomorrow's Implantable Electronic Systems. *EMBS 1996: "Bridging disciplines for biomedicine"*:497-498, 1996.

[30] Edell, D., and K. Gleason. Insulating Biomaterials NIH Contract #NO1-NS-9-2323. Bedford: InnerSea Technology, 1999.

[31] Edell, D. J. Development of a Chronic Neuroelectric Interface. In: *Biomedical Engineering*. Davis: University of California, 1980.

[32] Edell, D. J. A peripheral nerve information transducer for amputees: long-term multichannel recordings from rabbit peripheral nerves. *IEEE Trans. Biom. Eng.* 33:203-213, 1986.

[33] Edell, D. J., J. N. Churchill, and I. M. Gourley. Biocompatibility of a silicon based peripheral nerve electrode. *Biomat Med Dev Art Org* 10:103-122, 1982.

[34] Edell, D. J., V. V. Toi, V. M. McNeil, and L. D. Clark. Factors influencing the biocompatibility of insertable silicon microshafts in cerebral cortex. *IEEE Trans Biomed Eng* 39:635-43, 1992.

[35] Endo, L. P., N. L. Edwards, S. Lomgley, L. C. Corman, and R. S. Panuch. Silicone and rheumatic diseases. *Seminars in Arthritis and Rheumatism* 17:112-118, 1987.

[36] Forde, M., and P. Ridgely. Implantable Cardiac Pacemakers. In: *The Biomedical Engineering Handbook*, edited by J. D. Bronzino. Boca Raton: CRC Press, 1995.

[37] Goldblum, R. M., R. P. Pelley, A. A. O'Donell, D. Pyron, and J. P. Heggers. Antibodies to silicone elastomers and reactions to ventriculoperitoneal shunts. *Lancet* 340:510-513, 1992.

[38] Green, T. On death from chloroform; its prevention by galvanism. *British Medical Journal* 1:551-, 1872.

[39] Habal, M. B. The biologic basis for the clinical application of the silicones. *Arch. Surg* 119:843-848, 1984.

[40] Hayes, D., and e. al. Muilticenter experience with a bipolar tined polyurethane ventricular lead. *Pacing Clin Electrophysiol* 18:999-1004, 1995.

[41] Hetke, J. F., J. L. Lund, K. Najafi, K. D. Wise, and D. J. Anderson. Silicon ribbon cables for chronically implantable microelectrode arrays. *IEEE Trans Biomed Eng* 41:314-21, 1994.

[42] Hunt, J., M. J. G. Farthing, L. R. I. Baker, P. R. Crocker, and D. A. Levison. Silicone in the liver: possible late effects. *Gut* 30:239-242, 1989.

[43] Jones, L. Cable jacket aging study: comparison of polyether and polyester urethane materials. Albuquerque: Sandia Laboratories, 1977.

[44] Kovacs, G. T., C. W. Storment, and J. M. Rosen. Regeneration microelectrode array for peripheral nerve recording and stimulation. *IEEE Trans Biomed Eng* 39:893-902, 1992.

[45] Larson, B. C. *Design Considerations for Minimizing Noise in Micropower CMOS Integrated Circuits - Master's Thesis*. Cambridge: Massachusetts Institute of Technology, 1996. pp. 72.

[46] Lentini, J., and G. Severson. Humidity induced failures in parylene coated hybrids. *Circuits Manufacturing* May:56-57, 1984.

[47] Meyer, J.-U., H. Deutel, E. Valderrama, E. Cabruja, P. Aebischer, G. Soldani, and P. Dario. Perforated silicon dices with integrated nerve guidance channels for interfacing peripheral nerves. *IEEE Micro Electro Mechanical Systems*. IEEE, New York, NY, USA, 1995, p. 358-61.

[48] Najafi, K., J. Ji, and K. D. Wise. Scaling limitations of silicon multichannel recording probes. *IEEE Transactions on Biomed. Eng*. 37:1-11, 1990.

[49] Nelson, W. *Accelerated Testing*. New York: Wiley, 1990.

[50] Noll, W. *Chemistry and Technology of Silicones*. New York: Academic Press, 1968.

[51] Pine, J. Cultured Neuron Probe. Pasadena: California Institute of Technology, 1996.

[52] Roggendorf, E. The biostability of silicone rubbers, a polyamide and a polyester. *J. Biomed. Mater. Res.* 10:123-143, 1976.

[53] Rommel, M. L., A. S. Postyn, and T. A. Dyer. Accelerating Factors in Galvanically Induced Polyimide Degradation. *SAMPE Journal* 29:19-24, 1993.

[54] Rutten, W., H. vanWier, and J. Put. Sensitivity and selectivity of intraneural stimulation using a silicon electrode array. *IEEE Trans Biomed Eng* 38:192-198, 1991.

[55] Schmidt, P. F., and D. R. Wonsidler. Conversion of silicon nitride films to anodic silicon dioxide. *J. Elec. Chem. Soc.* 114:603-605, 1967.

[56] Seldon, H. L., M. C. Dahm, G. M. Clark, and S. Crowe. Silastic with polyacrylic acid filler: swelling properties, biocompatibility and potential use in cochlear implants. *Biomaterials* 15:1161-9, 1994.

[57] Sethi, K., N. Pandit, M. Bhargava, J. Mohan, R. Arora, and M. Khalilullah. Long term performance of silicone insulated and polyurethane insulated cardiac pacing leads. *Indian Heart* 44:145-149, 1992.

[58] Shepherd, R. K., R. L. Webb, G. M. Clark, B. C. Pyman, M. S. Hirshorn, M. T. Murray, and M. E. Houghton. Implanted material tolerance studies for a multiple-channel cochlear prosthesis. *411*:71-81, 1984.

[59] Tripp, T. B. The anodic oxidation of silicon nitride films on silicon. *J. Elec. Soc.* 117:157-159, 1970.

[60] Wallace, D. G., J. Rosenblatt, and G. A. Ksander. Tissue compatibility of collagen-silicone composites in a rat subcutaneous model. *Journal of Biomedical Materials Research* 26:1517-1534, 1992.

[61] Williams, D. *Concise Encyclopedia of Medical and Dental Materials*. Cambridge: MIT Press, 1990.

[62] Wise, K. D., J. B. Angell, and A. Starr. An integrated-circuit approach to extracellular microelectrodes. *IEEE Trans Biomed Eng* 17:238-47, 1970.